

PLANCK Component Separation using a Sparsity Prior

Jean-Luc Starck

CEA Saclay

Collaborators:

J. Bobin



F. Sureau

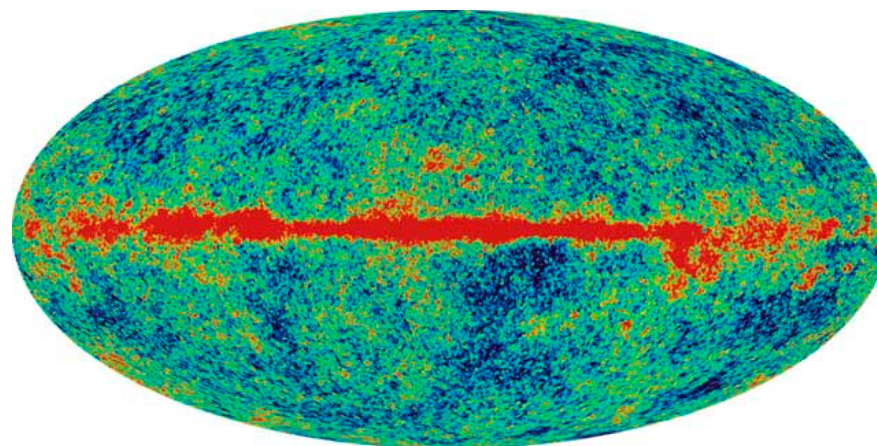
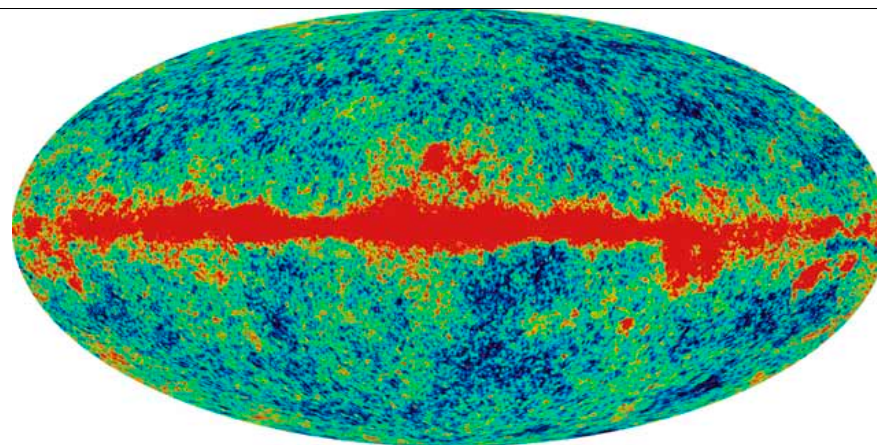
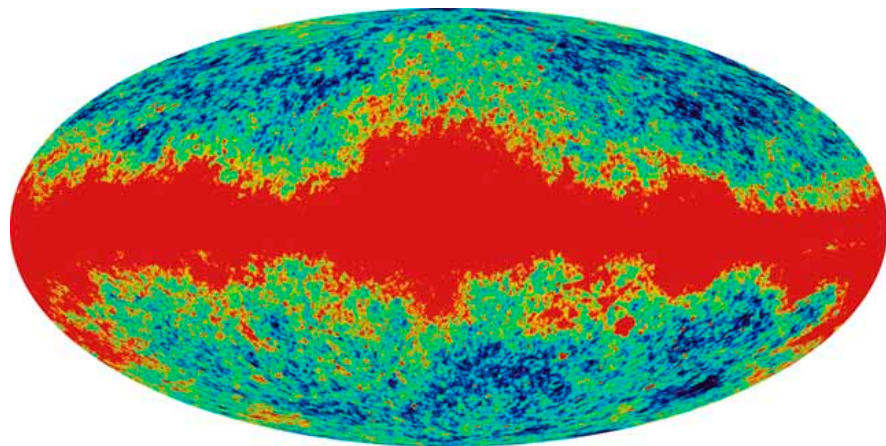


- Introduction
- Dictionaries on the Sphere
- Polarized Dictionaries on the Sphere
- Sparsity and Component Separation (temperature)
- Problems and new sparse approaches

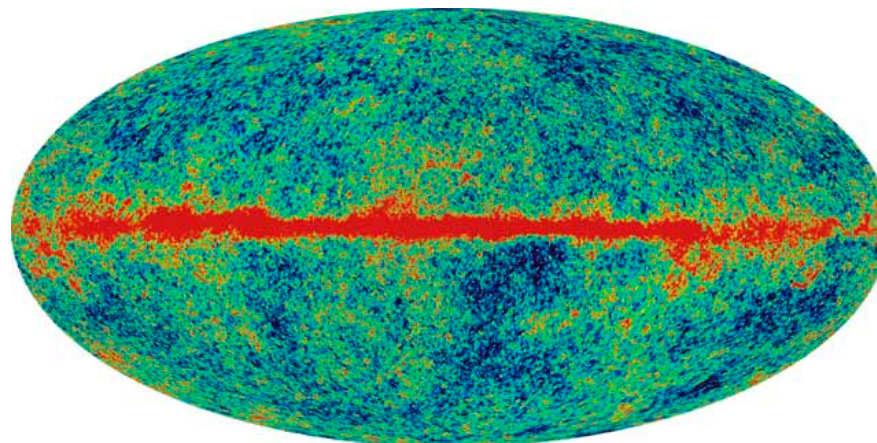
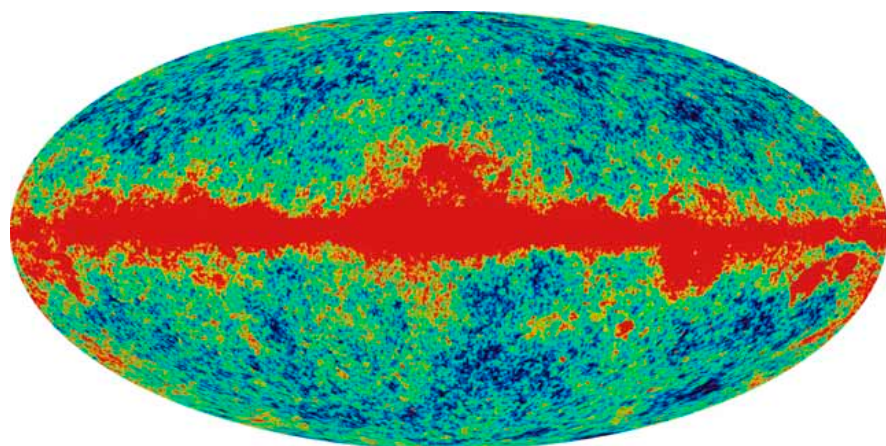
The Cosmic Microwave Background

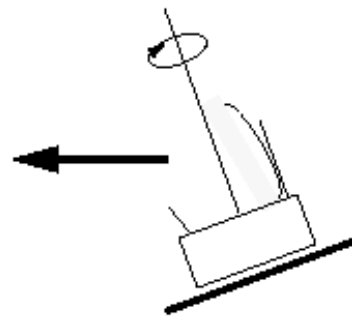
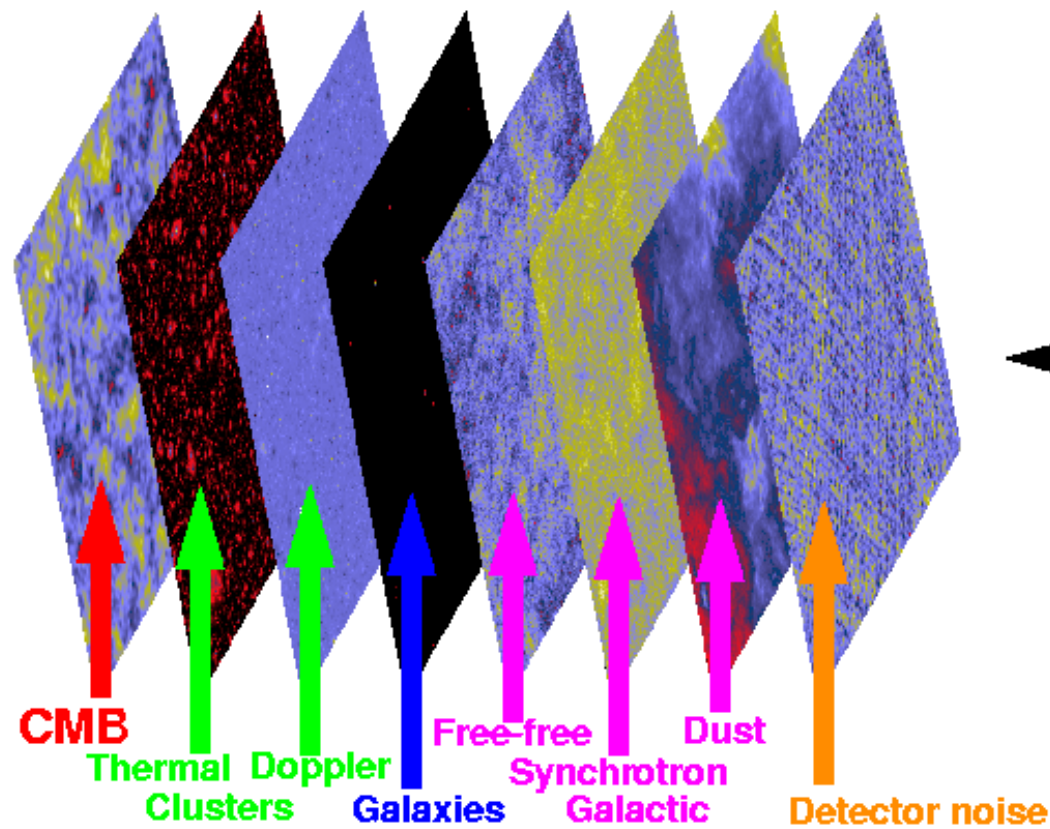
- The Universe is filled with a blackbody radiation field at a temperature of 3K.
- Predicted by G. Gamow in 1948
- Observed for the first time by Penzias and Wilson (1965)
- Confirmed by COBE (1990)
- Spectacular measurement of anisotropies by WMAP
- WMAP observed the CMB since 2002. Fifth and Last data release in August 2011.
- PLANCK first cosmological results in January 2013.

WMAP:five frequency maps

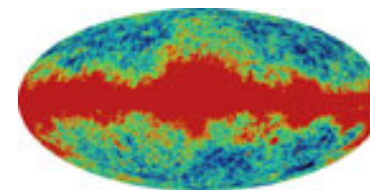


23, 33, 41, 61 and 93 GHz

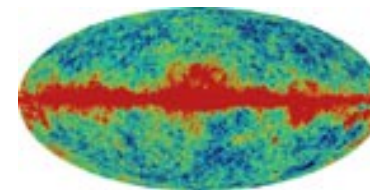




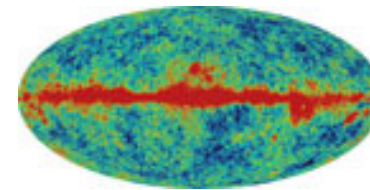
23 GHz



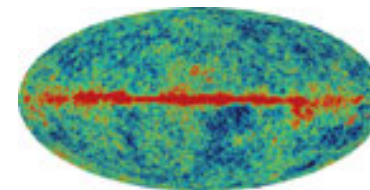
33 GHz



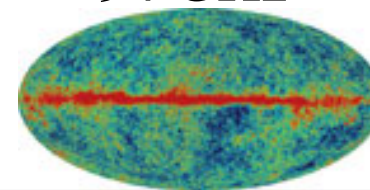
41 GHz



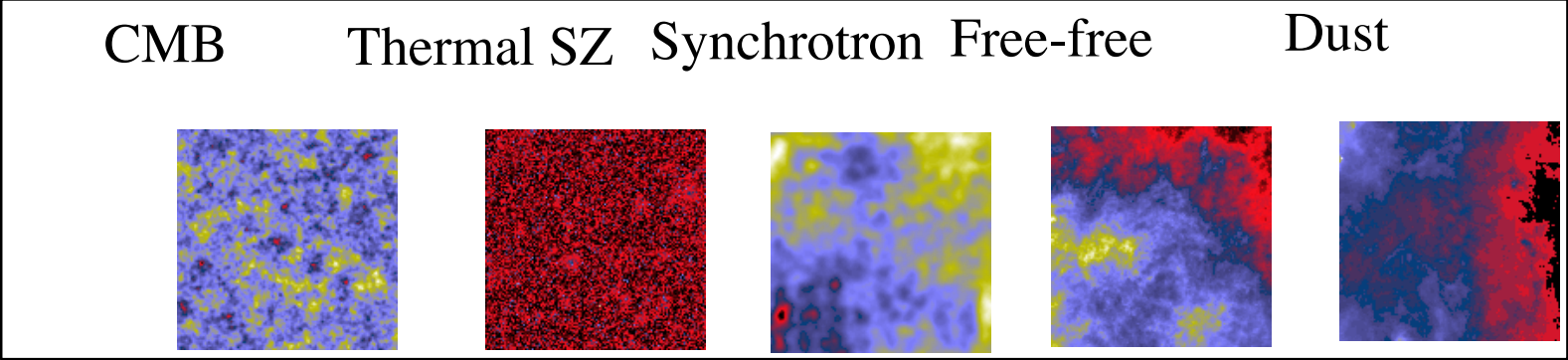
61 GHz



94 GHz



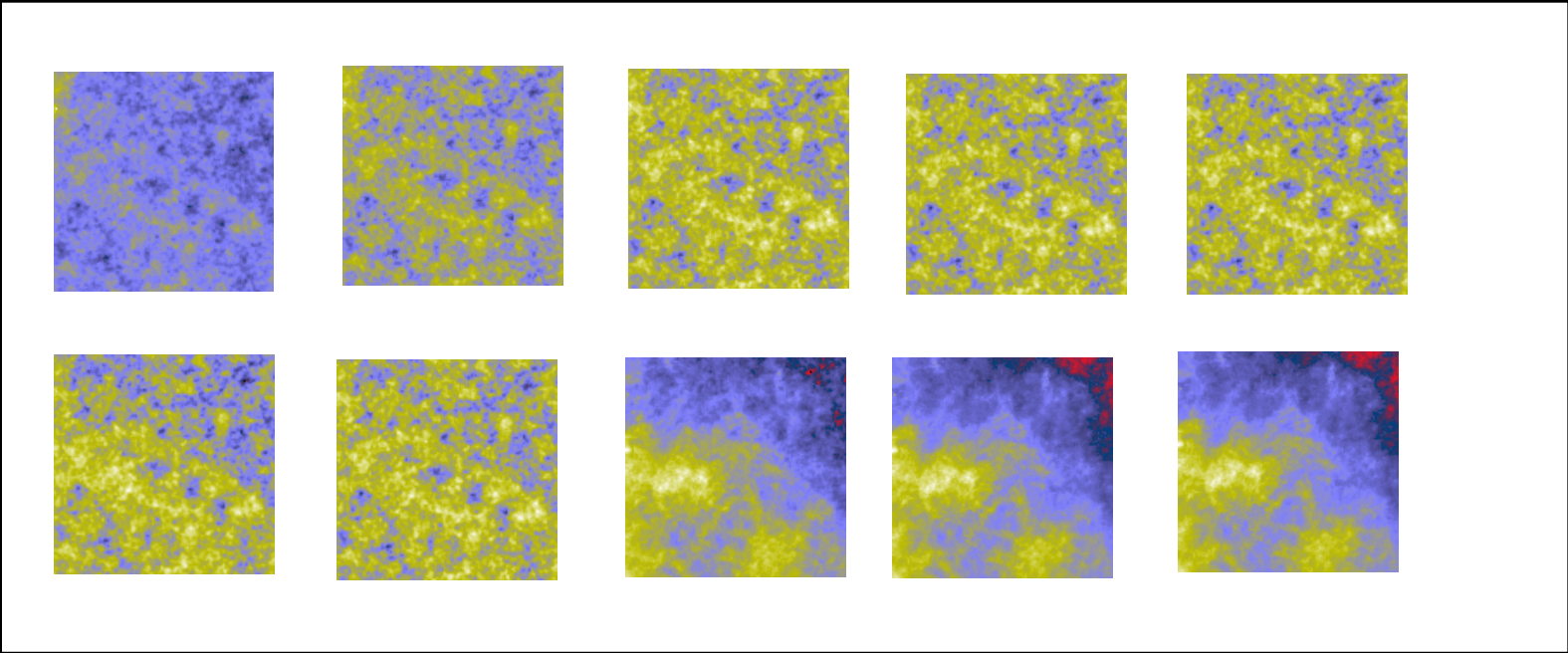
Synchrotron emission due to cosmic rays electrons accelerated into galactic magnetic fields



Sky components

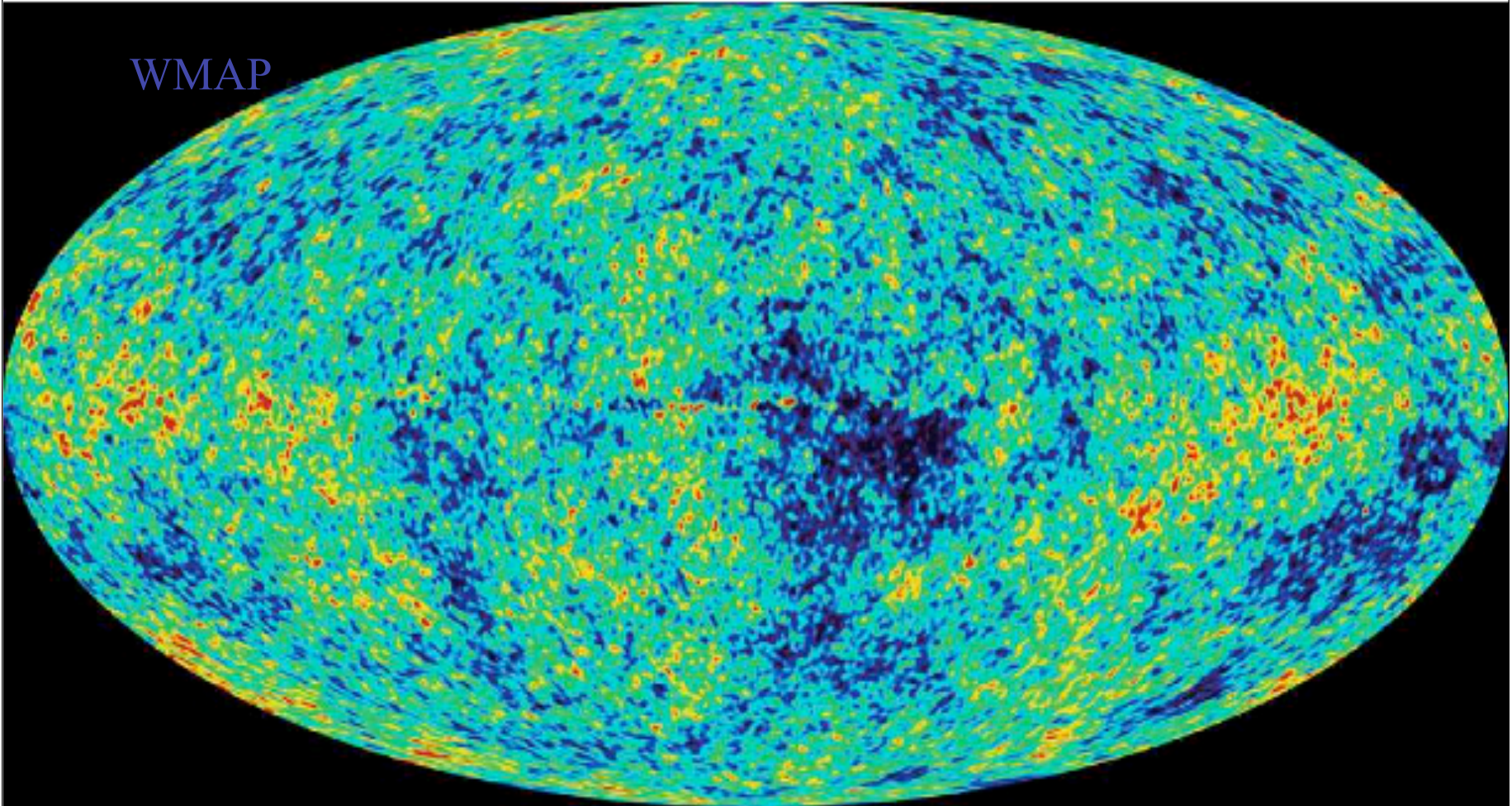
Linear combination + PSF + Noise

Observations



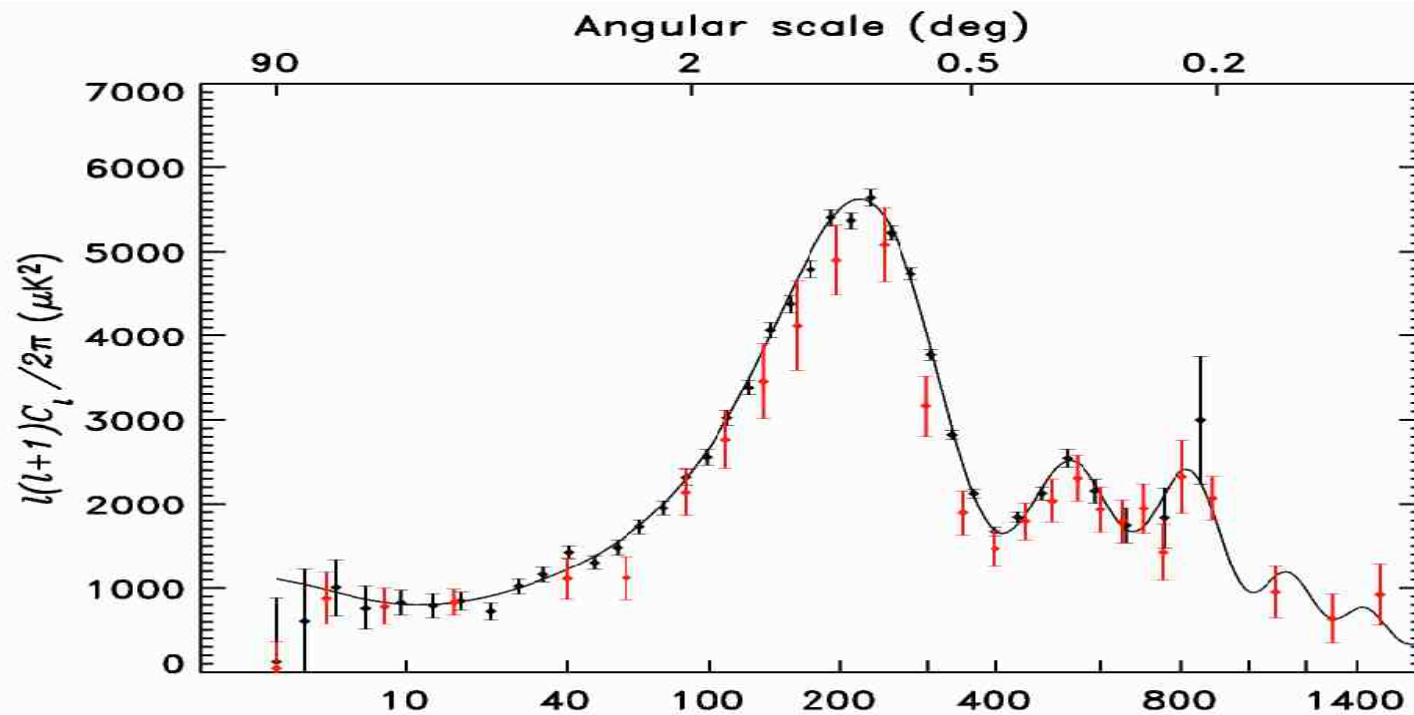
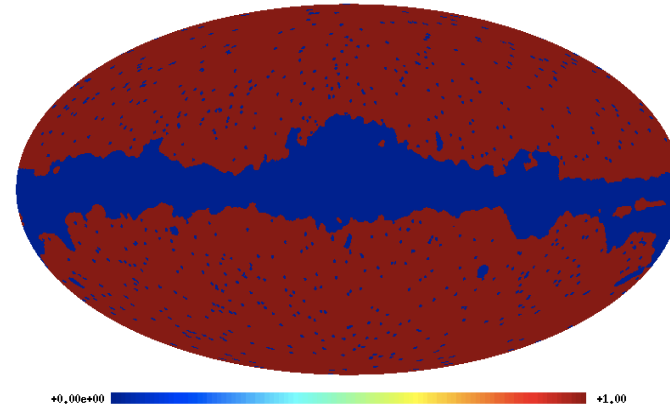
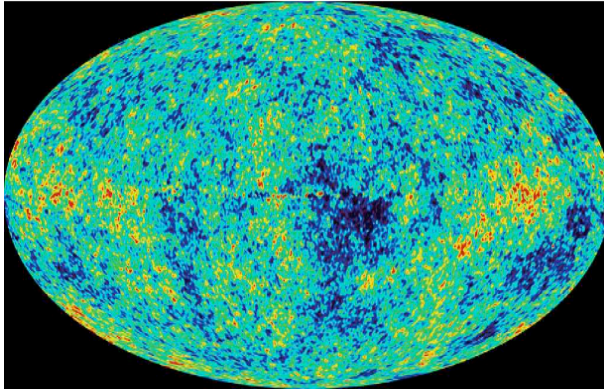
The CMB exhibits Fluctuations

WMAP



The Cosmic Microwave Background (CMB) is a relic radiation (with a temperature equals to 2.726 Kelvin) emitted 13 billion years ago when the Universe was about 370000 years old.

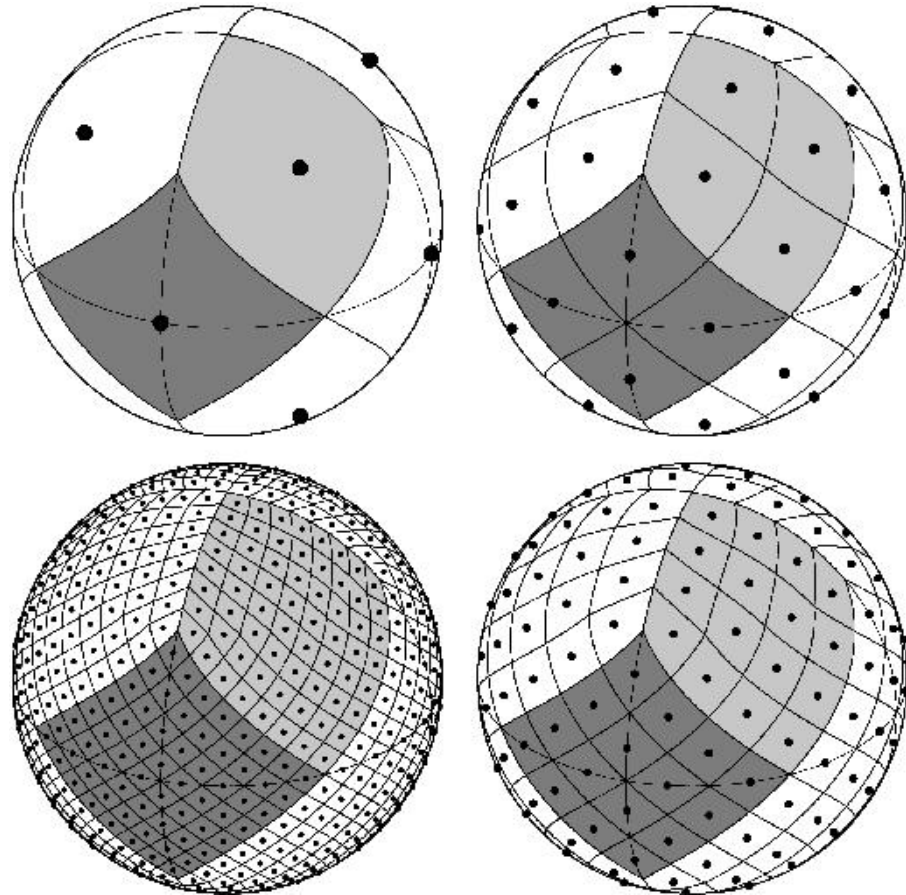
Power spectrum of WMAP

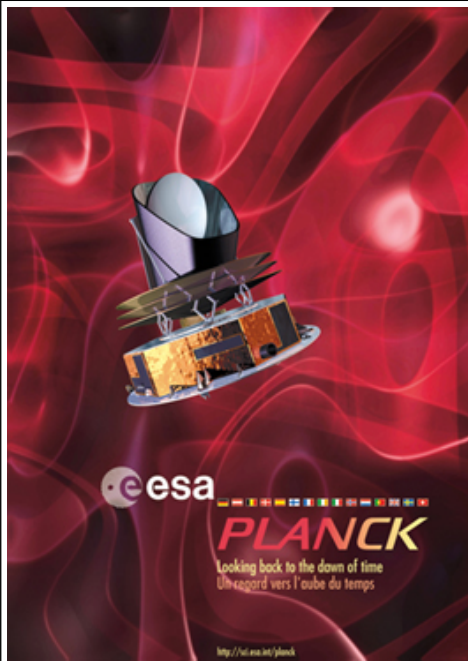


Healpix

K.M. Gorski et al., 1999, astro-ph/9812350,
<http://www.eso.org/science/healpix>

- Pixel = Rhombus
- Same Surfaces
- For a given latitude :
regularly spaced
- Number of pixels:
 $12 \times (N_{\text{sides}})^2$
- Included in the software:
 - Anafast
 - Synfast





Sparsity and PLANCK

- **Successor of WMAP (better resolution, better sensitivity, more channels)**
- **Launched on May 14, 2009**
- **Two instruments LFI and HFI**
- **Nine maps at 30,44,70,100,143,217,353,545,857 GHz**
- **Angular resolutions: 33', 24', 14', 10', 7.1', 5', 5', 5', 5'**

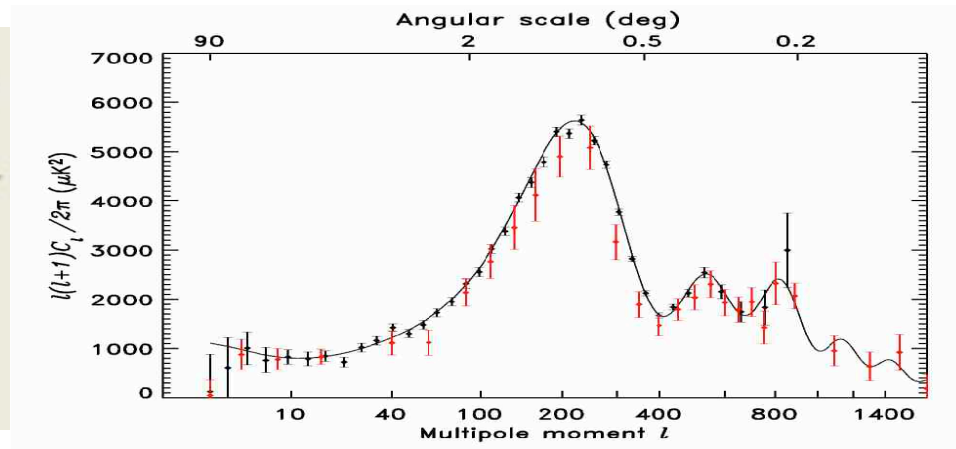
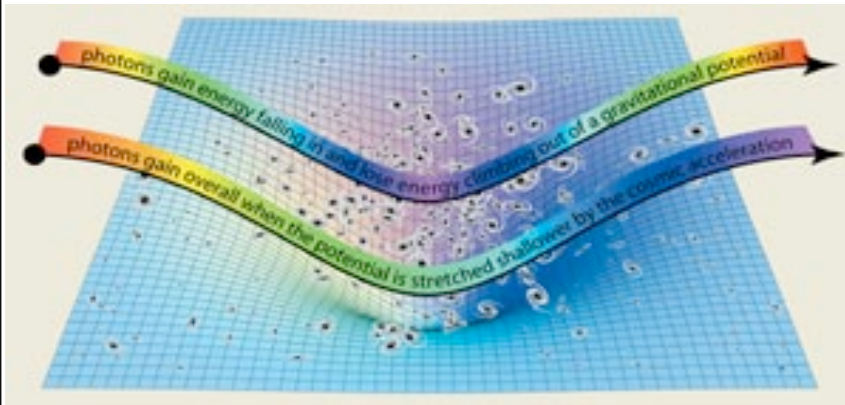
Many Cosmological Studies

Power spectrum \implies Cosmological parameters

CMB map is contaminated by non-Gaussianities

- Lensing effect: (L. Perotto, J. Bobin, S. Plaszczynski, J.-L. Starck and A. Lavabre "[Reconstruction of the CMB lensing for Planck](#)", A&A, 5109 A4, 2010.).
- Clusters of galaxies (SZ effect).
- Integrated Sachs Wolfe (ISW) effect

F.-X. Dupe, A. Rassat, J.-L. Starck, M. J. Fadili , "An Optimal Approach for Measuring the Integrated Sachs-Wolfe Effect", arXiv:1010.2192

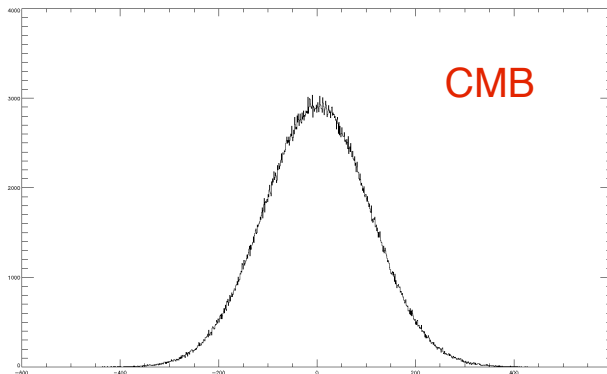
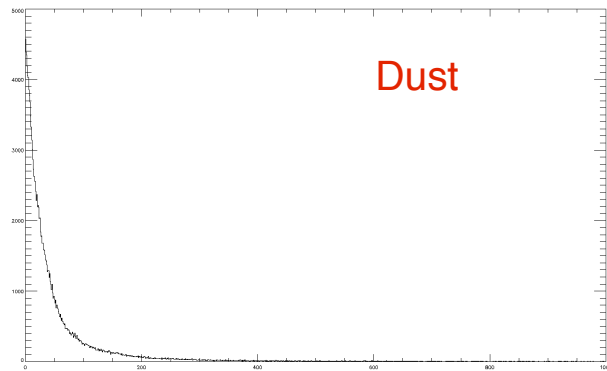


- Any other non-Gaussianity (Cosmic String, topology of the universe, etc)
- Is the CMB isotropic ?

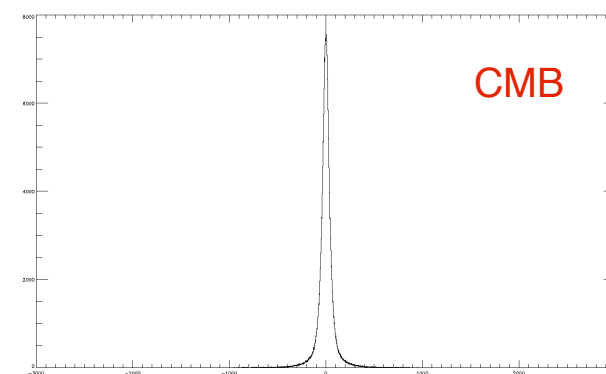
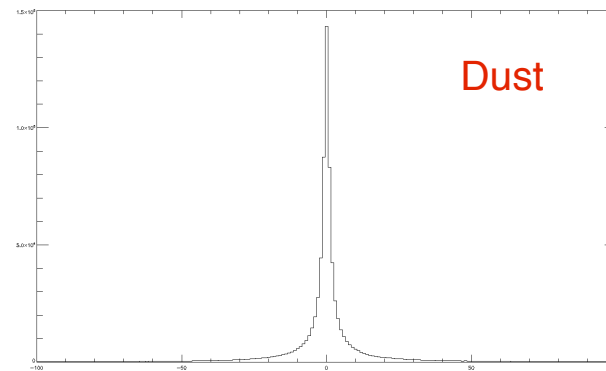
Strong Constraint: Sparsity

- Components are sparse in a wavelet dictionary

Spatial Domain

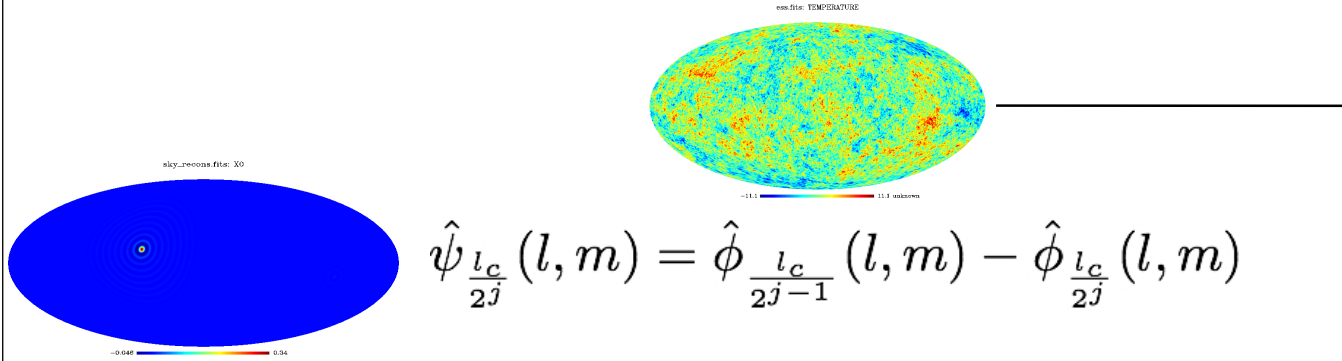


Wavelet Domain



Isotropic Undecimated Wavelet on the Sphere

Wavelets, Ridgelets and Curvelets on the Sphere, *Astronomy & Astrophysics*, 446, 1191-1204, 2006.



$$\hat{\psi}_{\frac{l_c}{2^j}}(l, m) = \hat{\phi}_{\frac{l_c}{2^{j-1}}}(l, m) - \hat{\phi}_{\frac{l_c}{2^j}}(l, m)$$

$$\hat{H}_j(l, m) = \begin{cases} \frac{\hat{\phi}_{\frac{l_c}{2^{j+1}}}(l, m)}{\hat{\phi}_{\frac{l_c}{2^j}}(l, m)} & \text{if } l < \frac{l_c}{2^{j+1}} \text{ and } m = 0 \\ 0 & \text{otherwise} \end{cases}$$

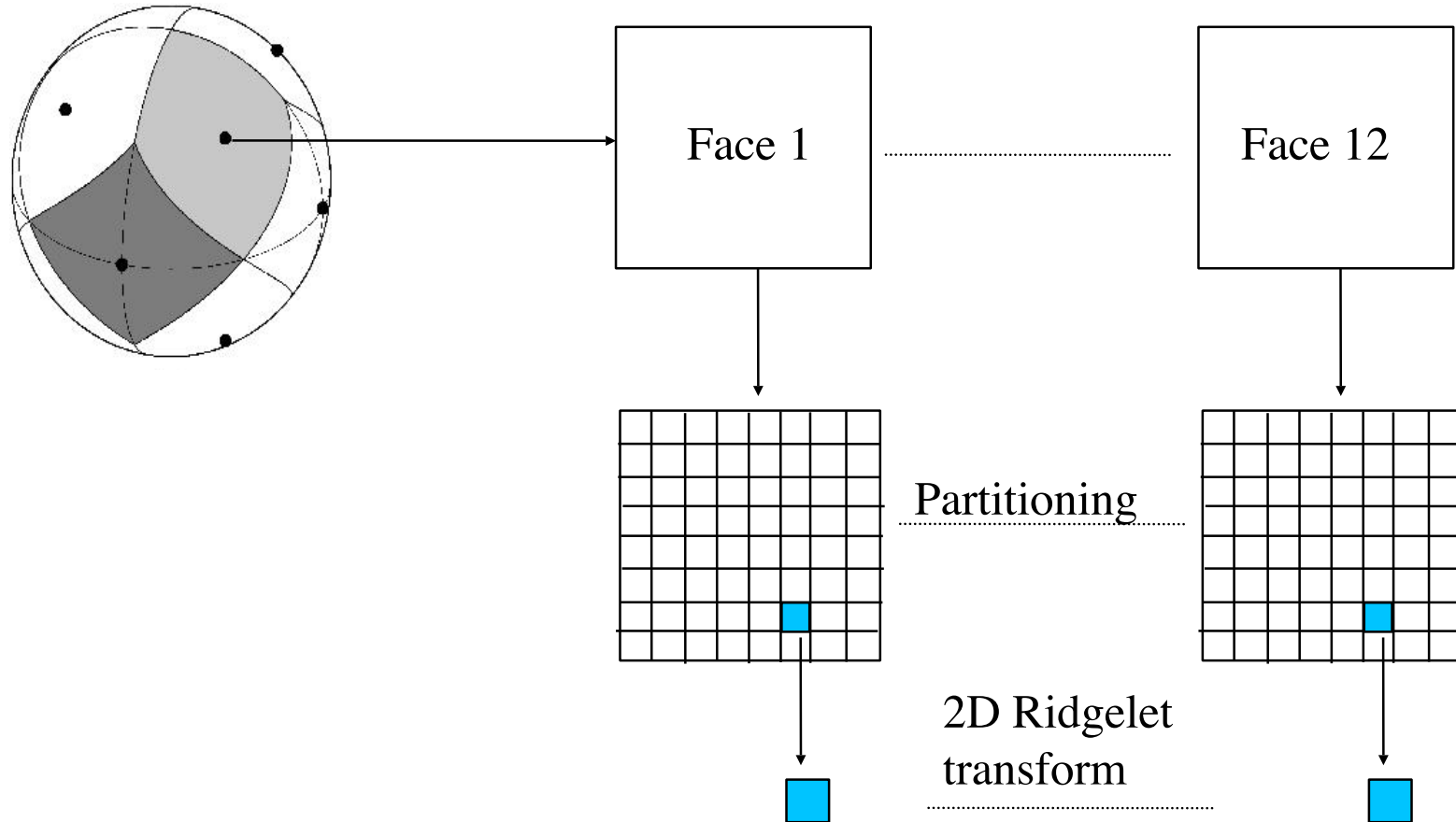
$$\hat{G}_j(l, m) = \begin{cases} \frac{\hat{\psi}_{\frac{l_c}{2^{j+1}}}(l, m)}{\hat{\phi}_{\frac{l_c}{2^j}}(l, m)} & \text{if } l < \frac{l_c}{2^{j+1}} \text{ and } m = 0 \\ 1 & \text{if } l \geq \frac{l_c}{2^{j+1}} \text{ and } m = 0 \\ 0 & \text{otherwise} \end{cases}$$

$$\hat{c}_{j+1}(l, m) = \hat{H}_j(l, m) \hat{c}_j(l, m)$$

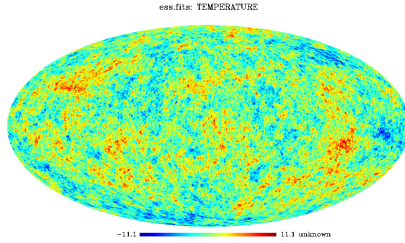
$$\hat{w}_{j+1}(l, m) = \hat{G}_j(l, m) \hat{c}_j(l, m)$$

$$c_0(\vartheta, \varphi) = c_J(\vartheta, \varphi) + \sum_{j=1}^J w_j(\vartheta, \varphi)$$

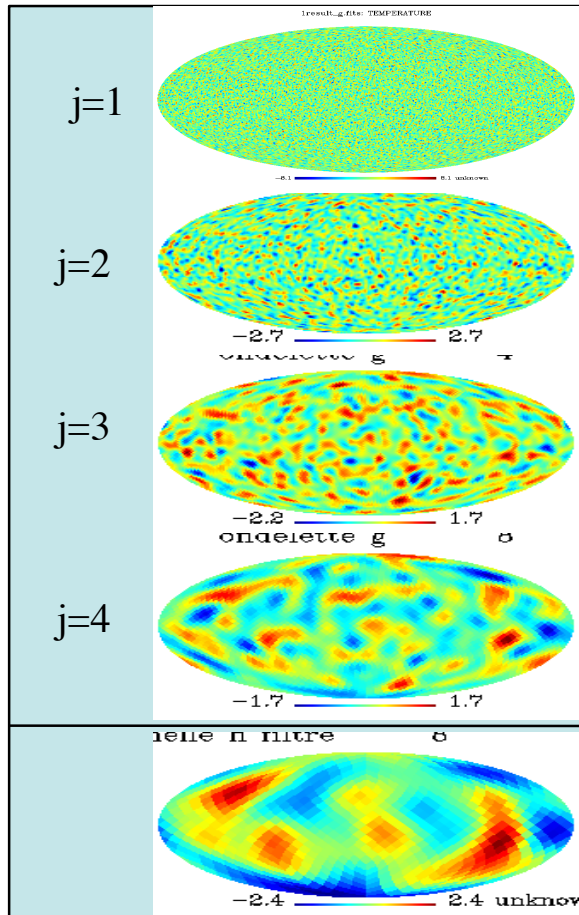
Ridgelets on the Sphere



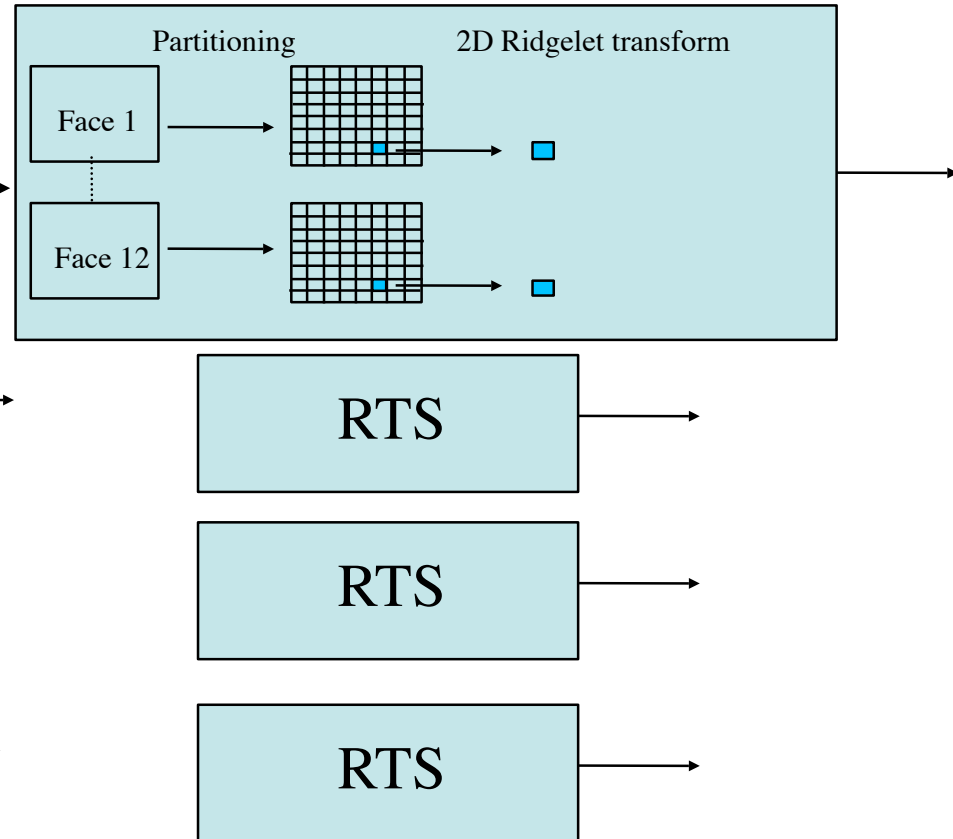
Curvelets on the Sphere



Pyramidal WT
on the Sphere

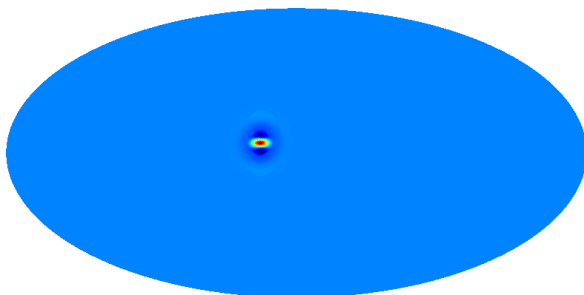


Ridgelet Transform on the Sphere (RTS)



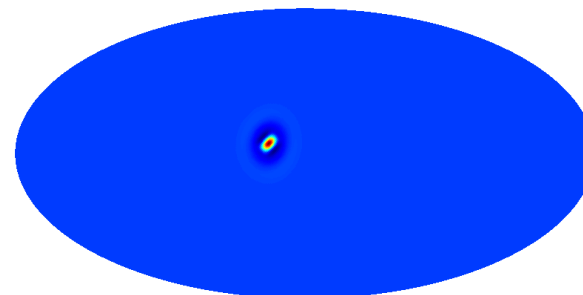
Example of curvelet functions on the sphere

on line processing :



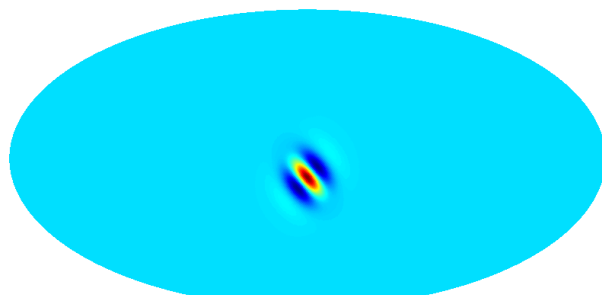
-0.054 0.16

on line processing :



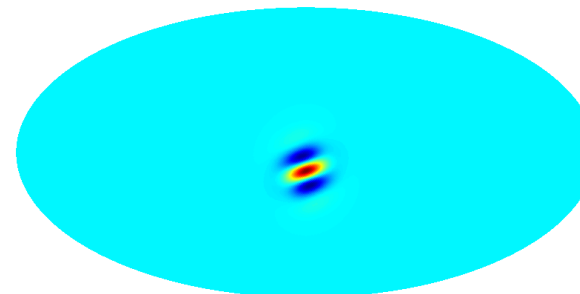
-0.028 0.17

on line processing :



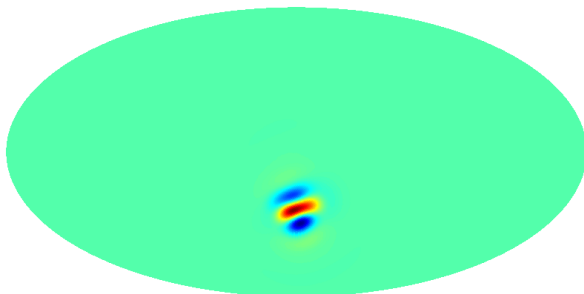
-0.018 0.036

on line processing :



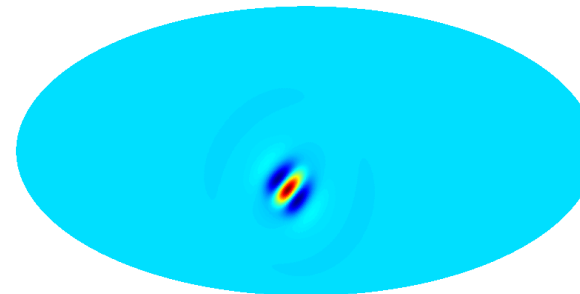
-0.012 0.020

on line processing :



-0.028 0.028

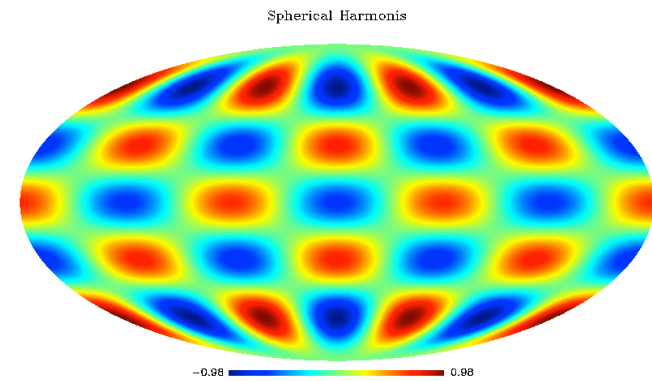
on line processing :



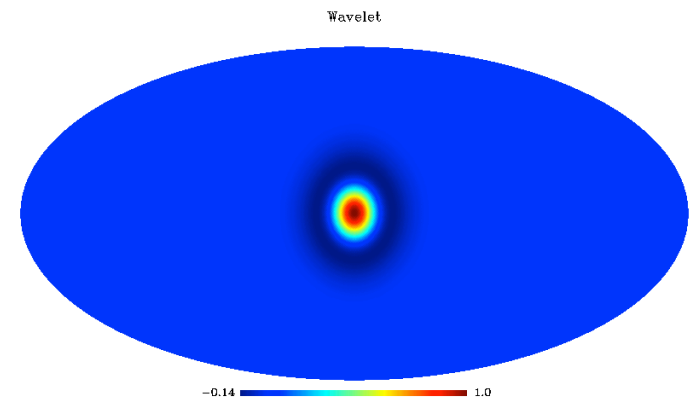
-0.016 0.038

Dictionaries

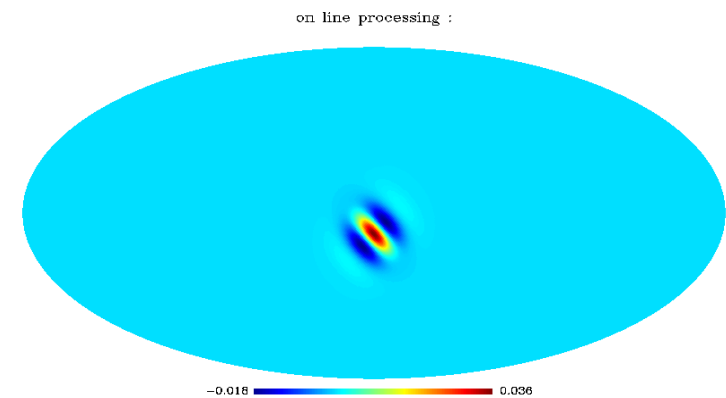
Spherical Harmonics



Wavelets



Curvelets



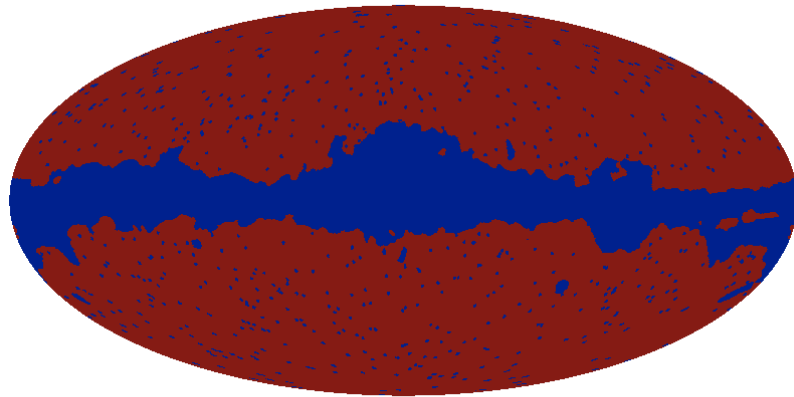
Interpolation of Missing Data: Sparse Inpainting

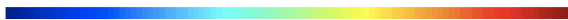
• M. Elad, J.-L. Starck, D.L. Donoho, P. Querre, "Simultaneous Cartoon and Texture Image Inpainting using Morphological Component Analysis (MCA)", *ACHA*, Vol. 19, pp. 340-358, 2005.

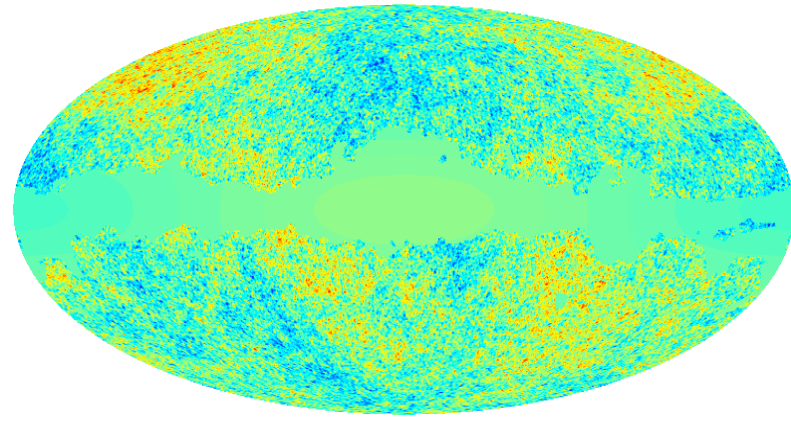
• P. Abrial, Y. Moudden, J.L. Starck, M.J. Fadili, J. Delabrouille, and M. Nguyen, "[CMB Data Analysis and Sparsity](#)", *Statistical Methodology*, Vol 5, No 4, pp 289-298, 2008.

$$\min_{\alpha} \|\alpha\|_p \quad \text{subject to} \quad Y = M\Phi\alpha$$

Where M is the mask: $M(i,j) = 0 \implies$ missing data
 $M(i,j) = 1 \implies$ good data



+0.00e+00  +1.00



-1.37e+03  +1.42e+03

Sparse-Inpainting preserves the ISW and the weak lensing signal.

L. Perotto, J. Bobin, S. Plaszczynski, J.-L. Starck, and A. Lavabre, "Reconstruction of the CMB lensing for Planck", *A&A*, 2010.

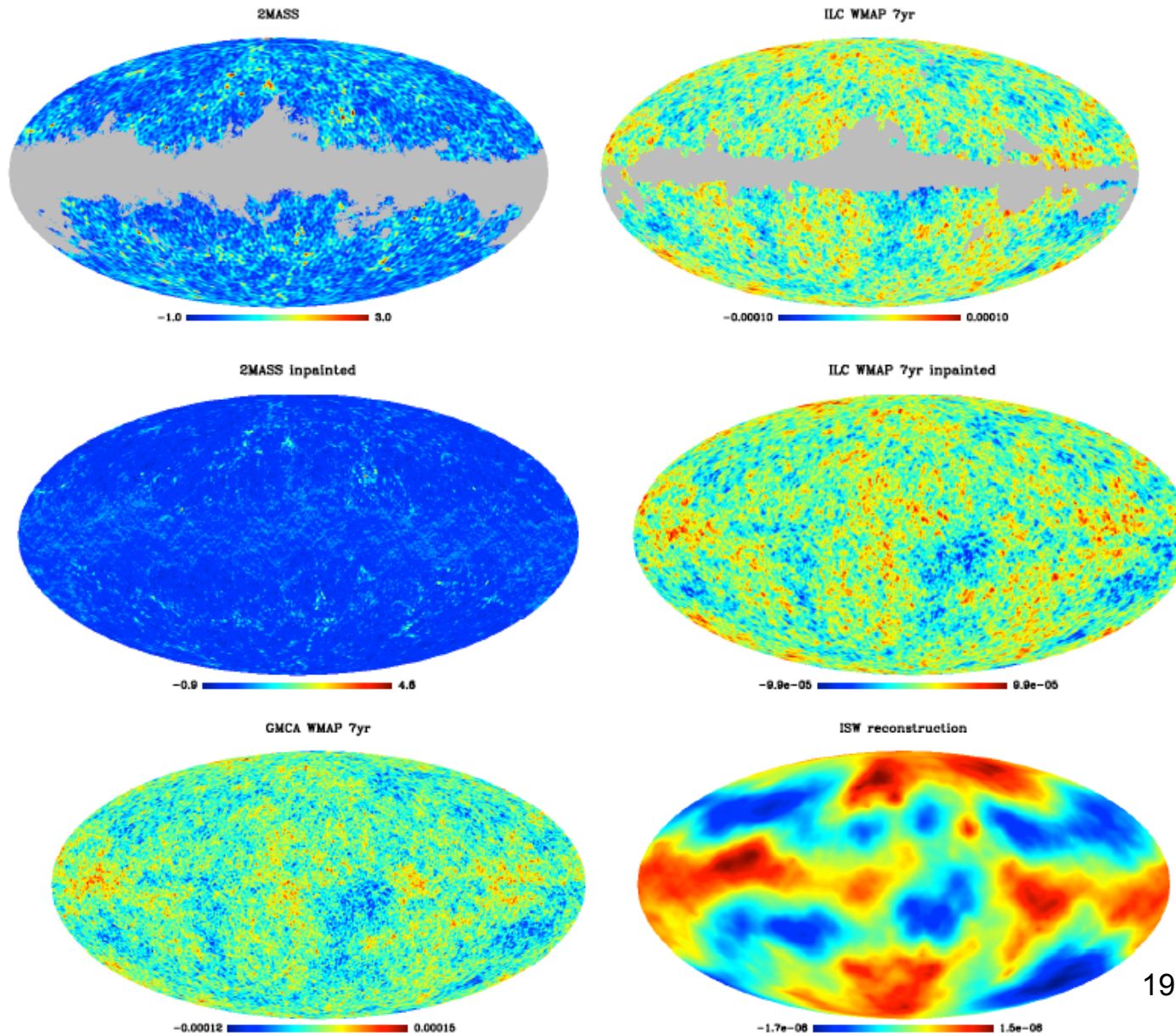
F.-X. Dupe, A. Rassat, J.-L. Starck, M. J. Fadili, "An Optimal Approach for Measuring the Integrated Sachs-Wolfe Effect", [arXiv:1010.2192](#)

Theoretical justification through the sampling theory of Compressed Sensing ?

Rauhut and Ward, "Sparse Legendre expansion via ℓ_1 minimization", *Constructive Approximation journal*, submitted.

ISW Detection

F.-X. Dupe, A. Rassat, J.-L. Starck, M. J. Fadili, "An Optimal Approach for Measuring the Integrated Sachs-Wolfe Effect", arXiv:1010.2192

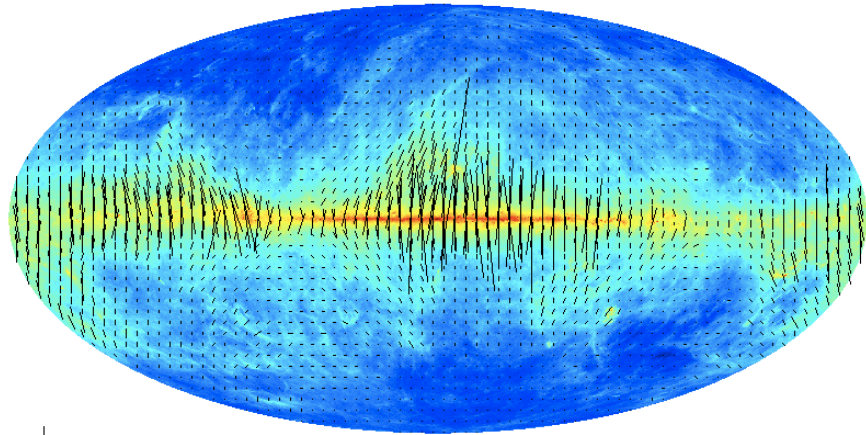


PLANCK POLARIZED DATA: T, Q, U

Magnitude $P = \sqrt{Q^2 + U^2}$

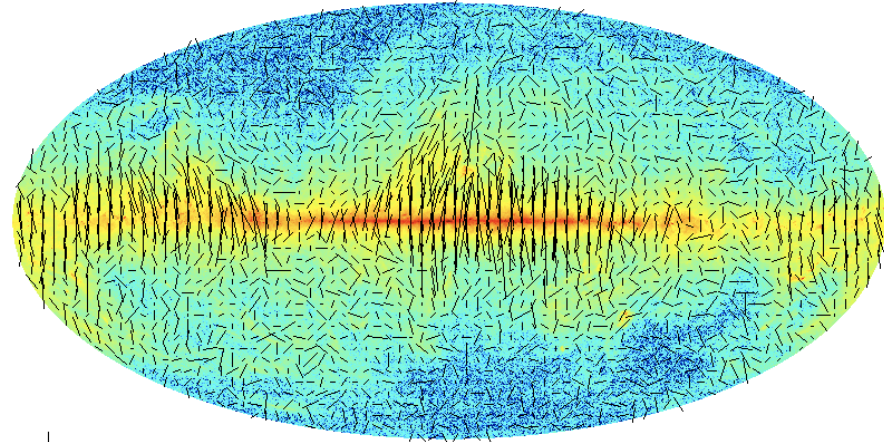
Orientation $\alpha = \arctan(U/Q)$

Dust 857 Ghz



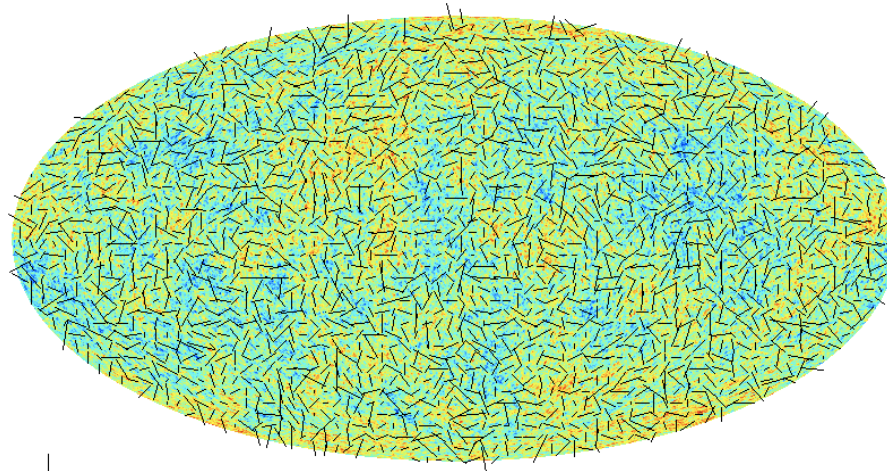
$5.0e-20 \text{ Log ()}$ -21. -16. Log ()

Dust 857 Ghz + noise



$5.0e-20 \text{ Log ()}$ -22.3 -16.3 Log ()

CMB

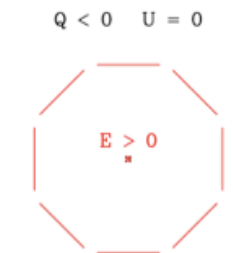
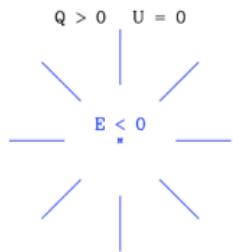


0.017 -0.50 0.50

E/B Mode Decomposition

$$E = \sum_{\ell,m} a_{\ell m}^E Y_{\ell m} = \sum_{\ell,m} -\frac{2a_{\ell m} + -2a_{\ell m}}{2} Y_{\ell m} \quad a_{\ell m}^E = -(a_{2,\ell m} + a_{-2,\ell m})/2$$

$$B = \sum_{\ell,m} a_{\ell m}^B Y_{\ell m} = \sum_{\ell,m} i\frac{2a_{\ell m} - -2a_{\ell m}}{2} Y_{\ell m} \quad a_{\ell m}^B = i(a_{2,\ell m} - a_{-2,\ell m})/2$$



$$Q = - \sum_{\ell,m} (a_{\ell,m}^E Z_{\ell,m}^+ + i a_{\ell,m}^B Z_{\ell,m}^-)$$

$$U = - \sum_{\ell,m} (a_{\ell,m}^B Z_{\ell,m}^+ - i a_{\ell,m}^E Z_{\ell,m}^-)$$

$$Z_{\ell,m}^+ = (2Y_{\ell,m} + -2Y_{\ell,m})/2$$

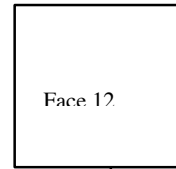
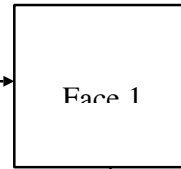
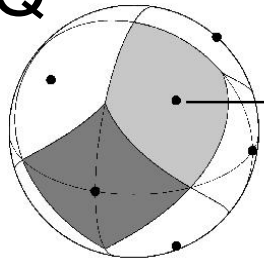
$$Z_{\ell,m}^- = (2Y_{\ell,m} - -2Y_{\ell,m})/2$$



E and B mode are closely related to the curl-free and div-free components of the vector field

Orthogonal Q-U Polarized Wavelet on the Sphere

Q

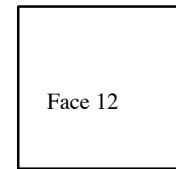
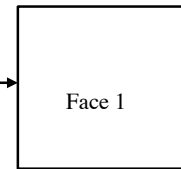
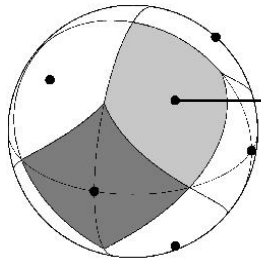


$\begin{matrix} j=0 \\ \hline j=1 \end{matrix}$	$\begin{matrix} h,0 \\ \hline h,1 \end{matrix}$	Horiz. Det. $j=1$	Horizontal Details $j=0$
$\begin{matrix} v,0 \\ \hline v,1 \end{matrix}$	$\begin{matrix} d,0 \\ \hline d,1 \end{matrix}$	Diag. Det. $j=1$	
Vertical Details $j=0$		Diagonal Details $j=0$	

$\begin{matrix} j=0 \\ \hline j=1 \end{matrix}$	$\begin{matrix} h,0 \\ \hline h,1 \end{matrix}$	Horiz. Det. $j=1$	Horizontal Details $j=0$
$\begin{matrix} v,0 \\ \hline v,1 \end{matrix}$	$\begin{matrix} d,0 \\ \hline d,1 \end{matrix}$	Diag. Det. $j=1$	
Vertical Details $j=0$		Diagonal Details $j=0$	

$$Q_k = \sum_p c_{J,p}^Q \phi_{j,k}(p) + \sum_p \sum_{j=1}^J \psi_{j,k}(p) w_{j,p}^Q$$

U



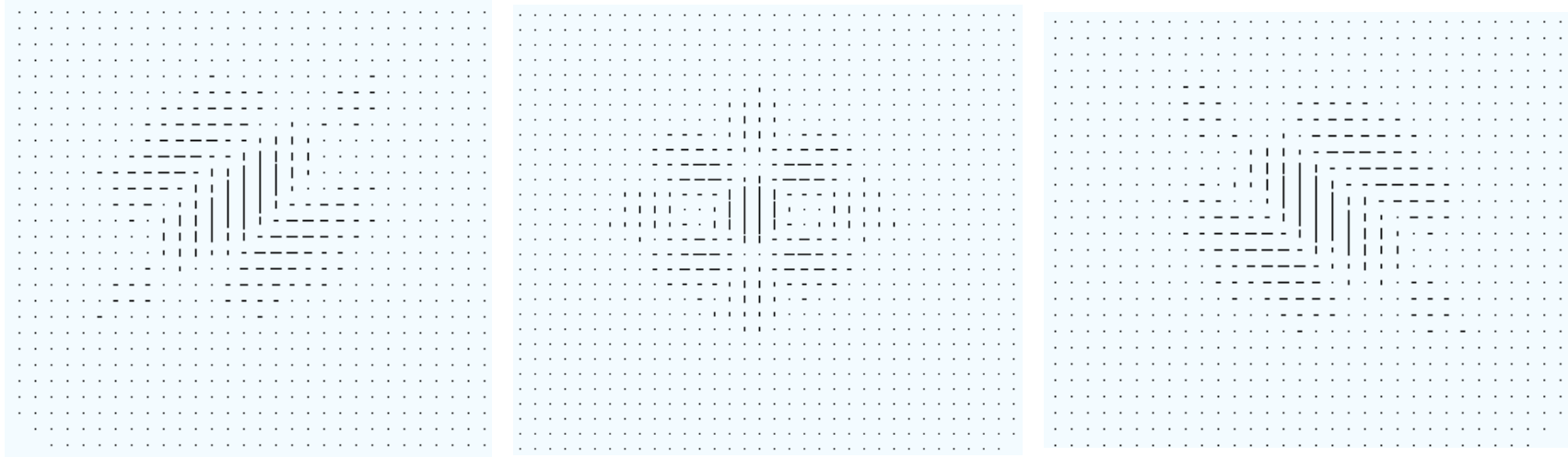
$\begin{matrix} j=0 \\ \hline j=1 \end{matrix}$	$\begin{matrix} h,0 \\ \hline h,1 \end{matrix}$	Horiz. Det. $j=1$	Horizontal Details $j=0$
$\begin{matrix} v,0 \\ \hline v,1 \end{matrix}$	$\begin{matrix} d,0 \\ \hline d,1 \end{matrix}$	Diag. Det. $j=1$	
Vertical Details $j=0$		Diagonal Details $j=0$	

$\begin{matrix} j=0 \\ \hline j=1 \end{matrix}$	$\begin{matrix} h,0 \\ \hline h,1 \end{matrix}$	Horiz. Det. $j=1$	Horizontal Details $j=0$
$\begin{matrix} v,0 \\ \hline v,1 \end{matrix}$	$\begin{matrix} d,0 \\ \hline d,1 \end{matrix}$	Diag. Det. $j=1$	
Vertical Details $j=0$		Diagonal Details $j=0$	

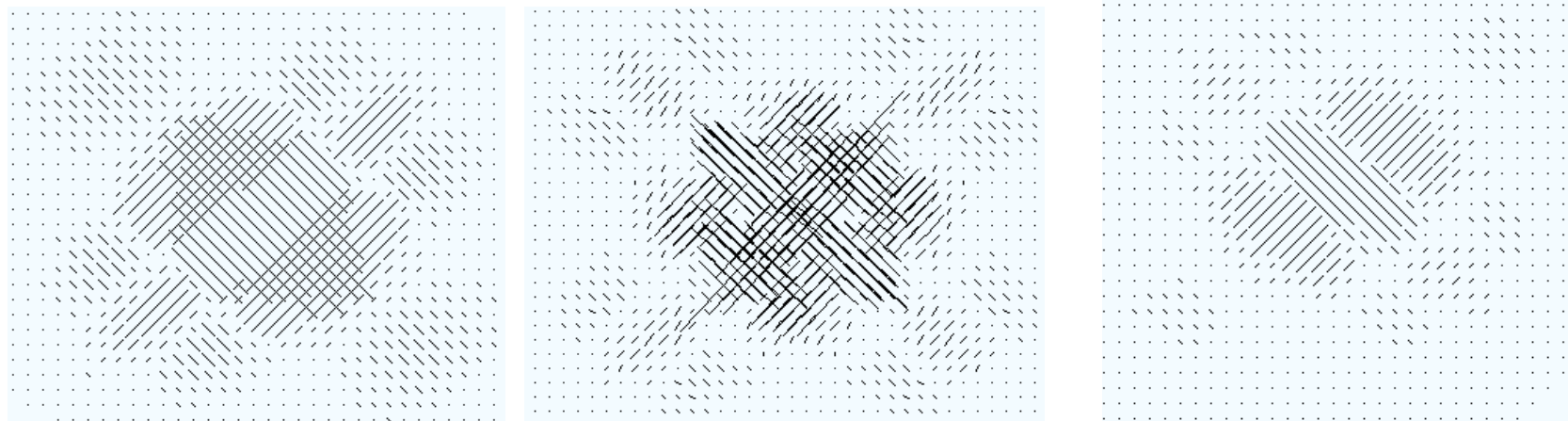
$$U_k = \sum_p c_{J,p}^U \phi_{j,k}(p) + \sum_p \sum_{j=1}^J \psi_{j,k}(p) w_{j,p}^U$$

$$(Q \pm iU)_k = \sum_p (c_{J,p}^Q \pm c_{J,p}^U) \phi_{j,k}(p) + \sum_p \sum_{j=1}^J \psi_{j,k}(p) (w_{j,p}^Q \pm w_{j,p}^U)$$

Q,U Orthogonal Wavelet Decomposition



Q-wavelet coefficient backprojection



U-wavelet coefficient backprojection

E/B Undecimated Wavelet Transform for Polarized Data

J.-L. Starck, Y. Moudden and J. Bobin, "Polarized Wavelets and Curvelets on the Sphere", Astronomy and Astrophysics, 497, 3, pp 931--943, 2009.

$$E = \sum_{\ell,m} a_{\ell m}^E Y_{\ell m} = \sum_{\ell,m} -\frac{2a_{\ell m} + -2a_{\ell m}}{2} Y_{\ell m}$$
$$B = \sum_{\ell,m} a_{\ell m}^B Y_{\ell m} = \sum_{\ell,m} i \frac{2a_{\ell m} - -2a_{\ell m}}{2} Y_{\ell m}$$

Wavelet Transform of E and B are obtained by:

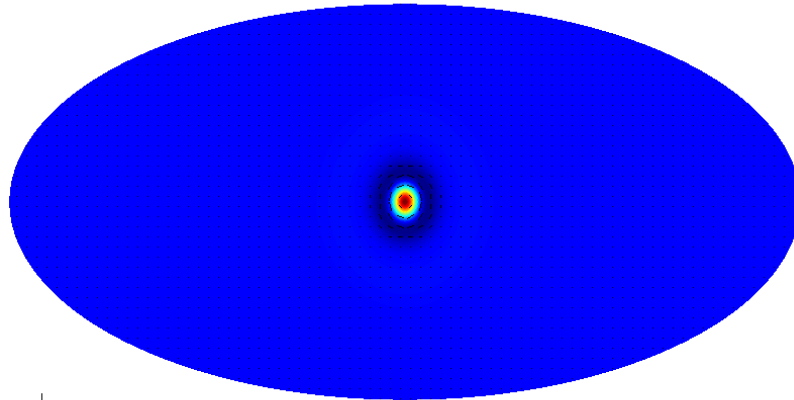
$$w_j^E = \langle E, \psi_j \rangle \quad w_j^B = \langle B, \psi_j \rangle$$

Furthermore, if we use the spherical isotropic wavelet construction of (starck et al, 2006), we have

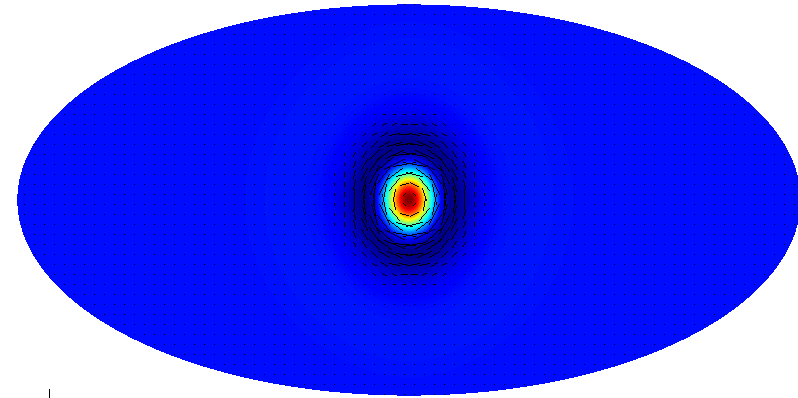
$$E(\theta, \phi) = c_J^E(\theta, \phi) + \sum_{j=1}^J w_j^E(\theta, \phi) \quad B(\theta, \phi) = c_J^B(\theta, \phi) + \sum_{j=1}^J w_j^B(\theta, \phi)$$

Wavelet and E/B Mode Decomposition

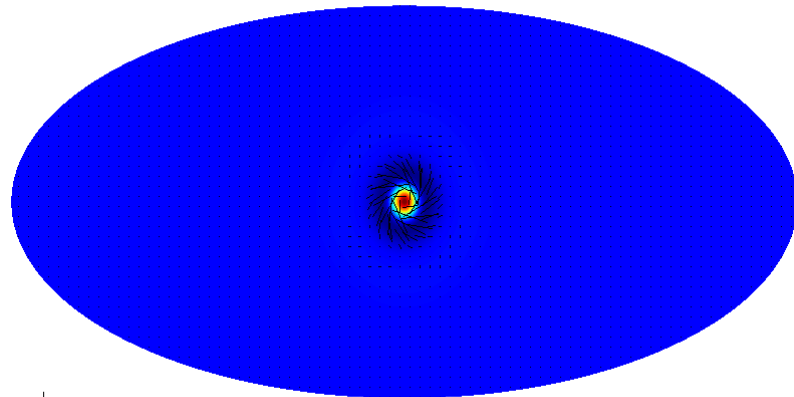
E-Wavelet Coefficient Backprojection (j=2)



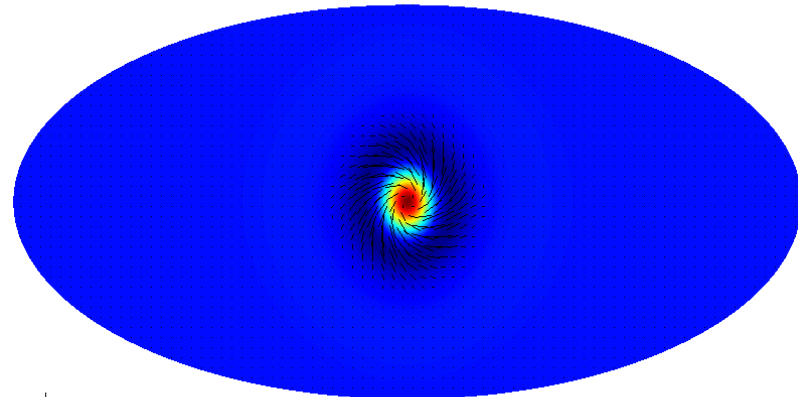
E-Wavelet Coefficient Backprojection (j=3)



B-Wavelet Coefficient Backprojection (j=2)



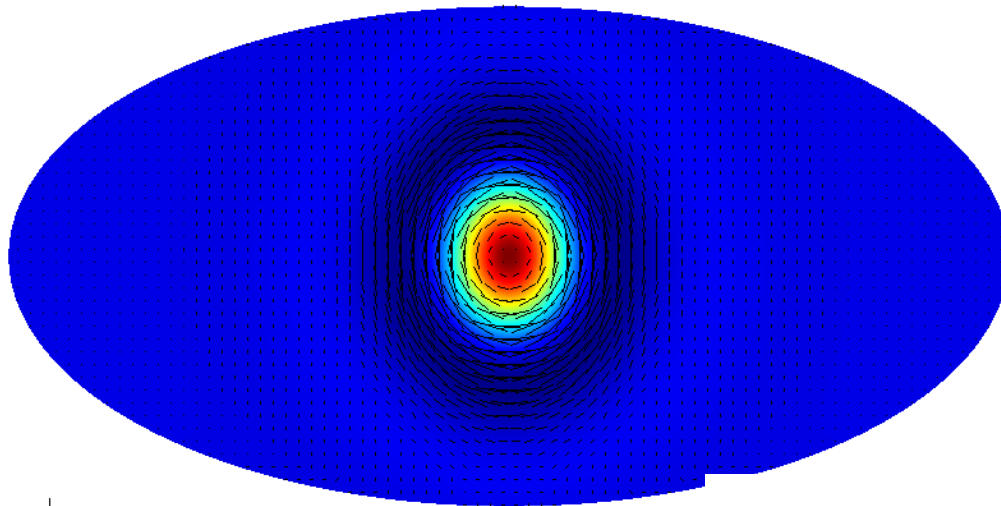
B-Wavelet Coefficient Backprojection (j=3)



Polarized Dictionary: E/B Polarized Wavelet

J.-L. Starck, Y. Moudden and J. Bobin, "Polarized Wavelets and Curvelets on the Sphere", Astronomy and Astrophysics, 497, 3, pp 931--943, 2009.

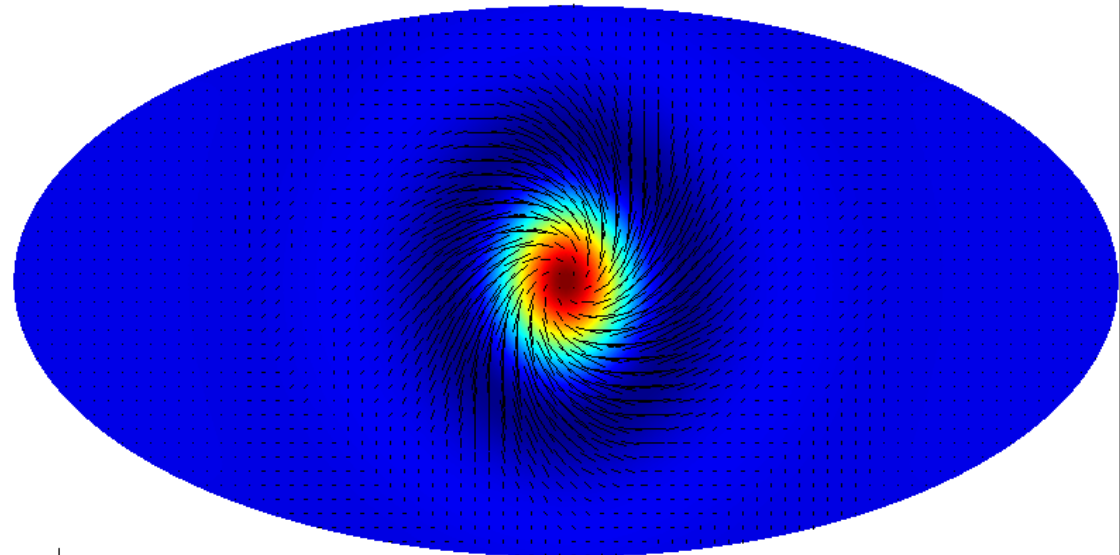
E-Wavelet Coefficient Backprojection



$j=4$

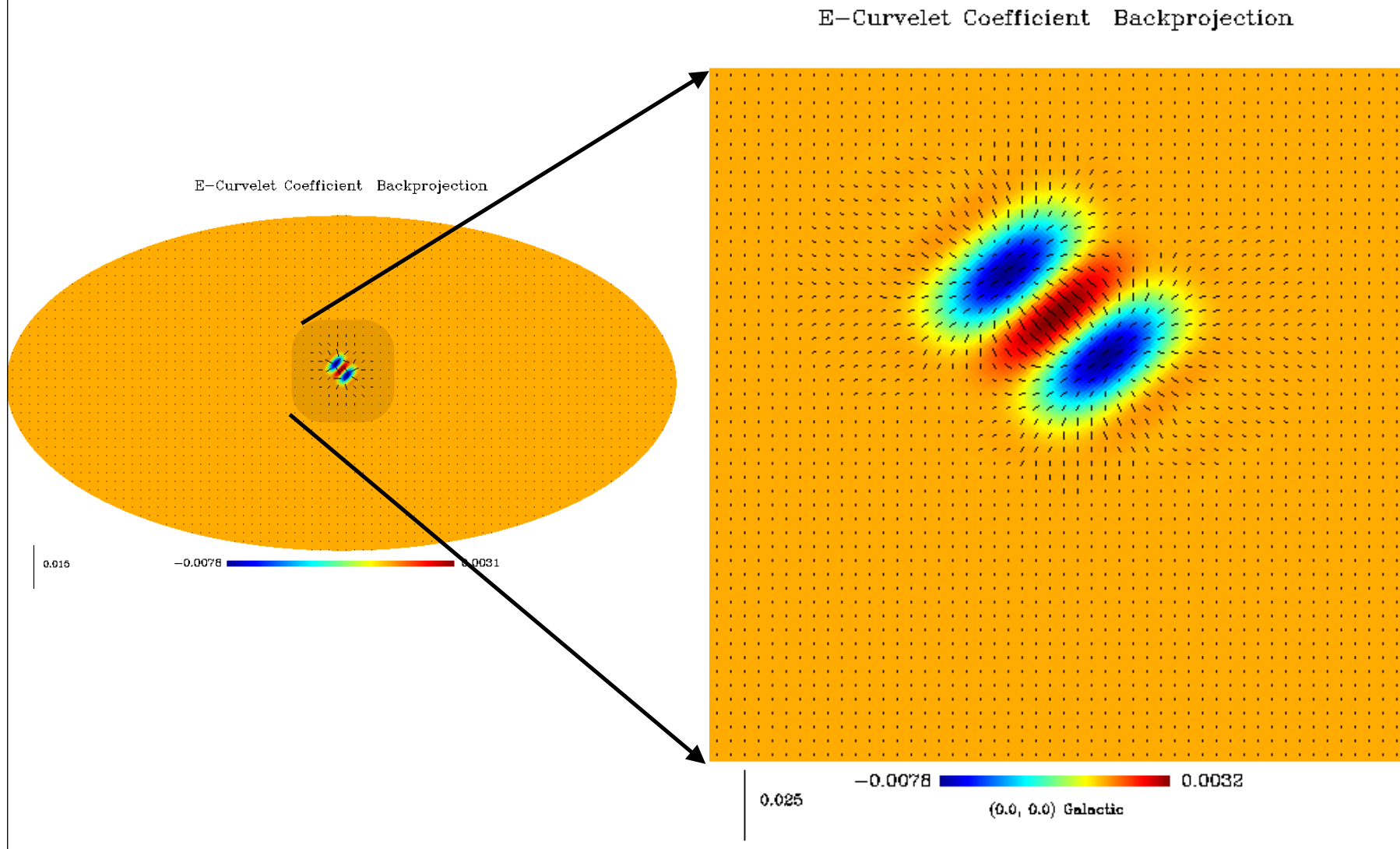
0.0050 -0.00087 0.00087

B-Wavelet Coefficient Backprojection

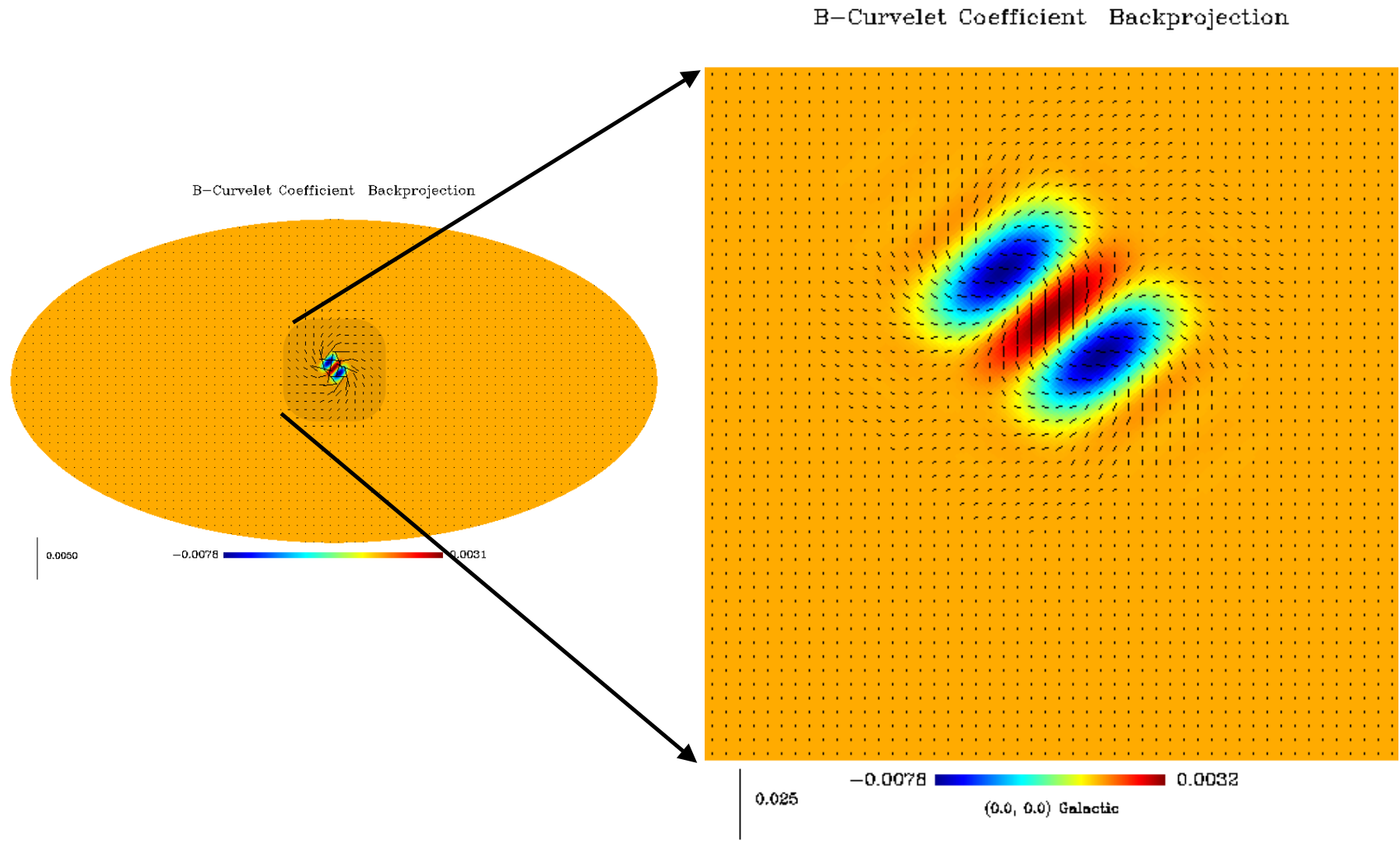


0.0050 -0.00087 0.00088

Curvelet and E/B Mode Decomposition



Curvelet and E/B Mode Decomposition



E/B Undecimated Wavelet Reconstruction

$$Q + iU = \sum_{lm} a_{2,lm} {}_2Y_{lm} \quad Q - iU = \sum_{lm} a_{-2,lm} {}_{-2}Y_{lm}$$

$$Q = -\frac{1}{2} \sum_{\ell,m} a_{\ell m}^E ({}_2Y_{\ell m} + {}_{-2}Y_{\ell m}) + ia_{\ell m}^B ({}_2Y_{\ell m} - {}_{-2}Y_{\ell m}) = \sum_{\ell,m} a_{\ell m}^E Z_{\ell m}^+ + ia_{\ell m}^B Z_{\ell m}^-$$

$$U = -\frac{1}{2} \sum_{\ell,m} a_{\ell m}^B ({}_2Y_{\ell m} + {}_{-2}Y_{\ell m}) - ia_{\ell m}^E ({}_2Y_{\ell m} - {}_{-2}Y_{\ell m}) = \sum_{\ell,m} a_{\ell m}^B Z_{\ell m}^+ - ia_{\ell m}^E Z_{\ell m}^-$$

As we have:
$$E = c_J^E + \sum_{j=1}^J w_j^E \quad \text{and} \quad B = c_J^B + \sum_{j=1}^J w_j^B$$

Then
$$Q(\theta, \phi) = \sum_{l,m} c_{J,l,m}^E Z_{l,m}^+ + ic_{J,l,m}^B Z_{l,m}^- + \sum_j \sum_{l,m} w_{j,l,m}^E Z_{l,m}^+ + iw_{j,l,m}^B Z_{l,m}^-$$

$$U(\theta, \phi) = \sum_{l,m} c_{J,l,m}^B Z_{l,m}^+ - ic_{J,l,m}^E Z_{l,m}^- + \sum_j \sum_{l,m} w_{j,l,m}^B Z_{l,m}^+ - iw_{j,l,m}^E Z_{l,m}^-$$

$$c_J^{X,+} = c_J^X \sum_{\ell,m} Y_{\ell m}^\dagger Z_{\ell m}^+ \quad \text{and} \quad c_J^{X,-} = c_J^X \sum_{\ell,m} Y_{\ell m}^\dagger Z_{\ell m}^-$$

Polarized Data Denoising

$$Q(\theta, \phi) = \sum_{l,m} c_{J,l,m}^E Z_{l,m}^+ + i c_{J,l,m}^B Z_{l,m}^- + \sum_j \sum_{l,m} \tilde{w}_{j,l,m}^E Z_{l,m}^+ + i \tilde{w}_{j,l,m}^B Z_{l,m}^-$$

$$U(\theta, \phi) = \sum_{l,m} c_{J,l,m}^B Z_{l,m}^+ - i c_{J,l,m}^E Z_{l,m}^- + \sum_j \sum_{l,m} \tilde{w}_{j,l,m}^B Z_{l,m}^+ - i \tilde{w}_{j,l,m}^E Z_{l,m}^-$$

Where

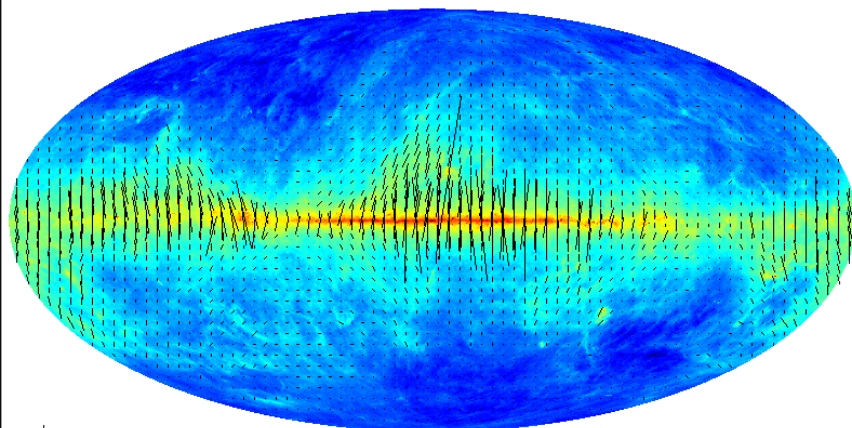
$$\tilde{w}_{j,k}^E = \delta(w_{j,k}^E)$$
$$\tilde{w}_{j,k}^B = \delta(w_{j,k}^B)$$

Hard thresholding corresponds to the following non linear operation:

$$\tilde{w}_{j,k} = \begin{cases} w_{j,k} & \text{if } |w_{j,k}| \geq T_j \\ 0 & \text{otherwise} \end{cases}$$

Polarized Data Denoising

Dust 857 Ghz

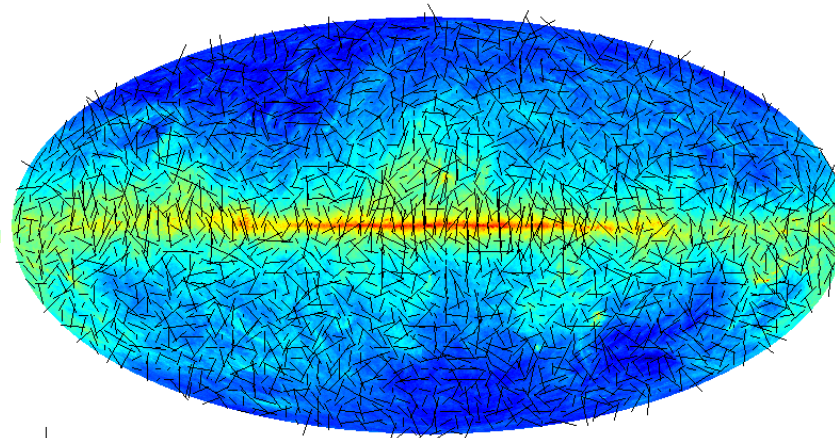


20.0 Log ()

-0.51

4.2 Log ()

Dust 857 Ghz + noise

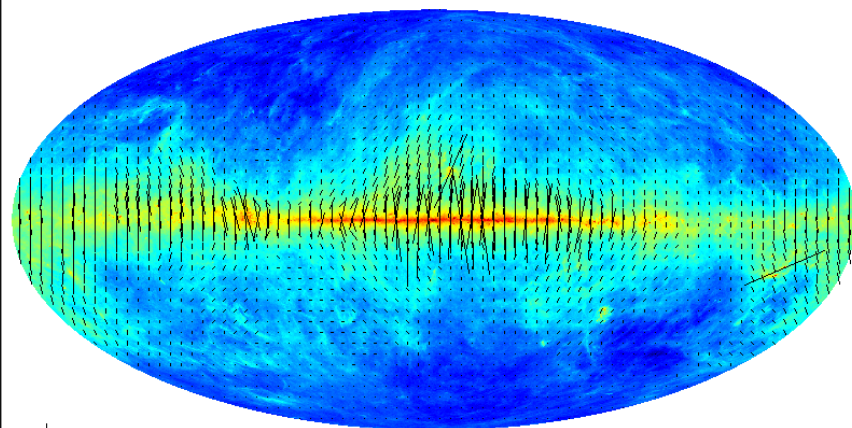


40.0 Log ()

-0.51

4.2 Log ()

E-B Wavelet filtering

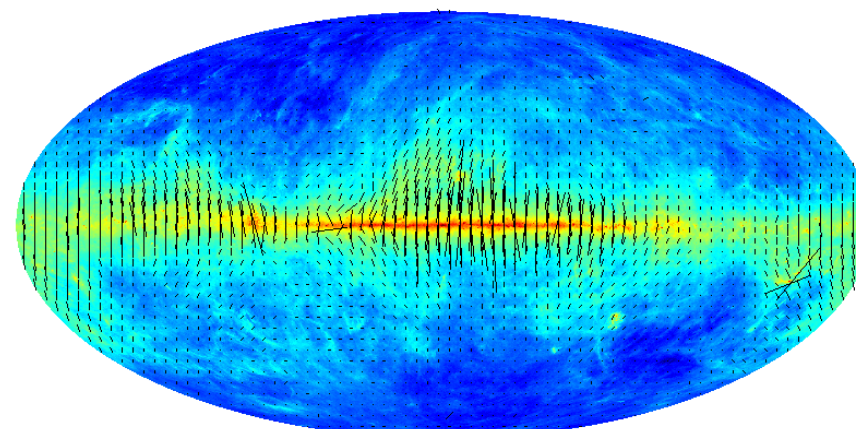


20.0 Log ()

-0.51

4.2 Log ()

E-B Curvelet Denoising



20.0 Log ()

-0.51

4.2 Log ()

MRS Version V2.0 available since June 2010

Wavelet, Ridgelet and Curvelet on the Sphere :

Software available at: <http://jstarck.free.fr/mrs.html>

J.-L. Starck, P. Abrial, Y. Moudden and M. Nguyen, *Wavelets, Ridgelets and Curvelets on the Sphere*, *Astronomy & Astrophysics*, 446, 1191-1204, 2006.

1. Wavelet transforms
 - Continuous Wavelet Transform (Mexican Hat)
 - Orthogonal Wavelets
 - Undecimated isotropic wavelet transform (Spline, Meyer and Needlet filters).
 - Pyramidal wavelet transform
2. Ridgelet and Curvelet Transforms
3. Denoising using Wavelets and Curvelets
4. Gaussianity tests: Skewness, Kurtosis, Moment of order 5 and 6, Max, Higher Criticism
5. Astrophysical Component Separation (ICA on the Sphere): JADE, Fast ICA, GMCA.
6. Sparse Inpainting.

Polarized Spherical Wavelets and Curvelets: SparsePol/Version 1.0

Software available at: <http://jstarck.free.fr/mrsp.html>

J.-L. Starck, Y. Moudden and J. Bobin, "Polarized Wavelets and Curvelets on the Sphere", *Astronomy and Astrophysics*, 497, 3, pp 931--943, 2009.

Morpho-Spectral Diversity

Data: $X = [x_1, \dots, x_m]$

Source: $S = [s_1, \dots, s_n]$

$$X = [x_1, \dots, x_m] = AS$$

$$x_l = \sum_{i=1}^n a_{i,l} s_i$$

$$\min_{\alpha} \|\alpha\|_p \text{ s.t. } \mathbf{X} = \sum_{\gamma \in \Gamma} \alpha_{\gamma} \psi_{\gamma}$$

$$\Phi_{\mathbf{A}} = [\Phi_{\mathbf{A},1}, \Phi_{\mathbf{A},2}]$$

$$\Phi_{\mathbf{S}}$$

Spatial Dictionary with
Spectral Dictionary

$$\Psi = [\Phi_{\mathbf{A},1} \otimes \Phi_{\mathbf{S}}, \Phi_{\mathbf{A},2} \otimes \Phi_{\mathbf{S}}]$$

Sparse Component Separation Method:

Generalized Morphological Analysis Method (GMCA)

- J. Bobin, J.-L. Starck, M.J. Fadili, and Y. Moudden, "Sparsity, Morphological Diversity and Blind Source Separation", IEEE Trans. on Image Processing, Vol 16, No 11, pp 2662 - 2674, 2007.
- J. Bobin, J.-L. Starck, M.J. Fadili, and Y. Moudden, "[Blind Source Separation: The Sparsity Revolution](#)", Advances in Imaging and Electron Physics, Vol 152, pp 221 -- 306, 2008.



$$\text{Source: } X = [x_1, x_n] \quad \text{Data: } Y = [y_1, \dots, y_n] = AX + N$$

We define a dictionary ϕ

⇒

GMCA searches a sparse solution X in the dictionary ϕ subject to the constraint that the norm $\|Y - AX\|^2$ is minimal.

GMCA + sky model : we can easily introduce in the component separation a priori knowledge in order to improve the separation.

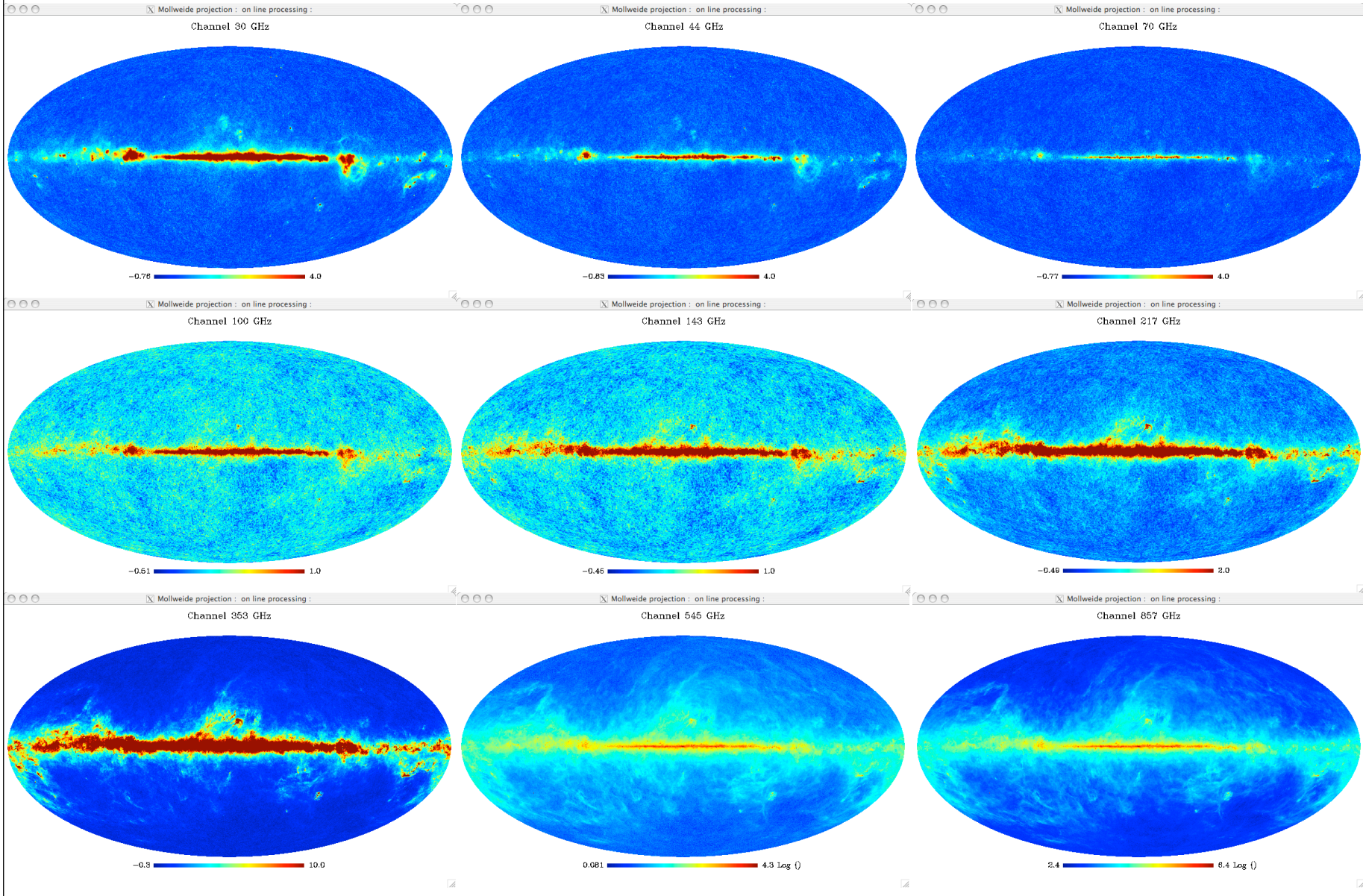
• J. Bobin, Y. Moudden, J.-L. Starck, M.J. Fadili, and N. Aghanim, "[SZ and CMB reconstruction using GMCA](#)", Statistical Methodology, astro-ph/0712.0588, 2008.

- CMB, SZ: The spectrum is known
- Free-Free: The spectrum is known up to a scale factor.

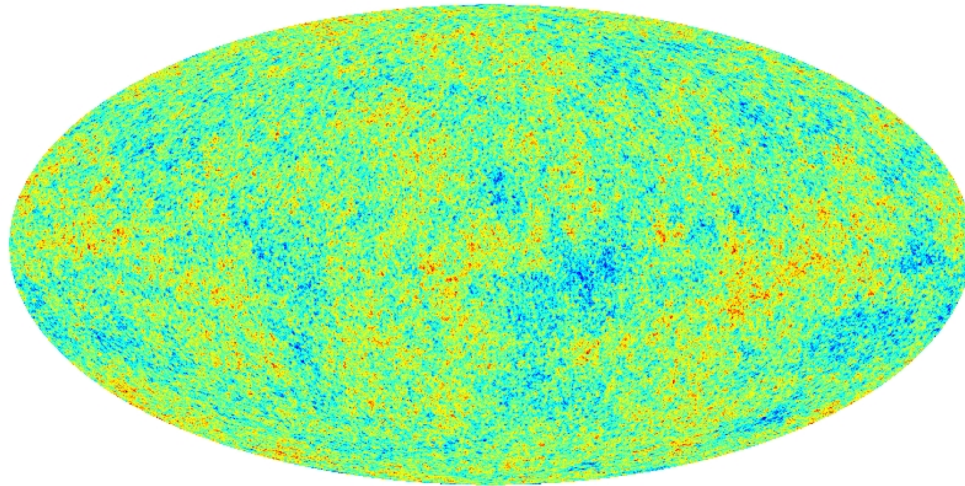
We have nine channels and we search for nine sources:

3 sources are modeled (CMB, SZ, Free-Free) and 6 are not modeled.

PLANCK Simulated Data

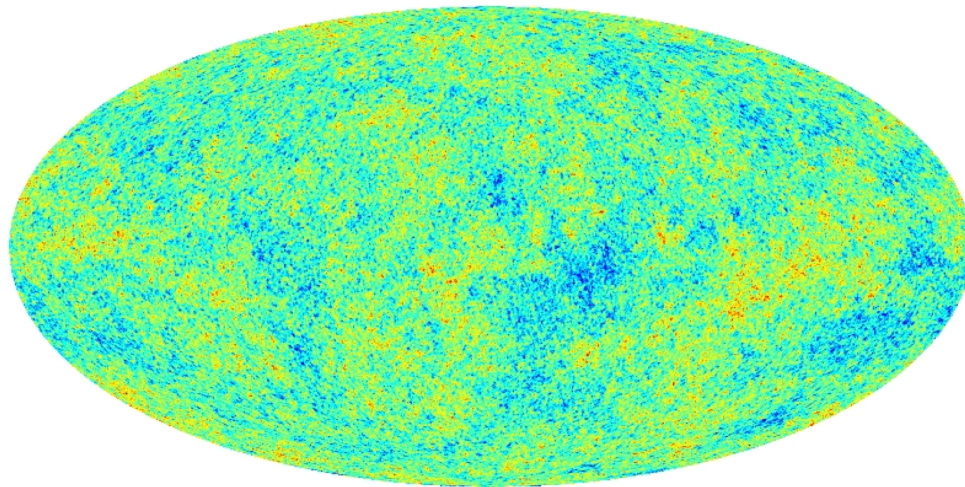


Planck - WG2 - Challenge 2



-0.50 0.50

Input simulated CMB map (mK)



-0.50 0.50

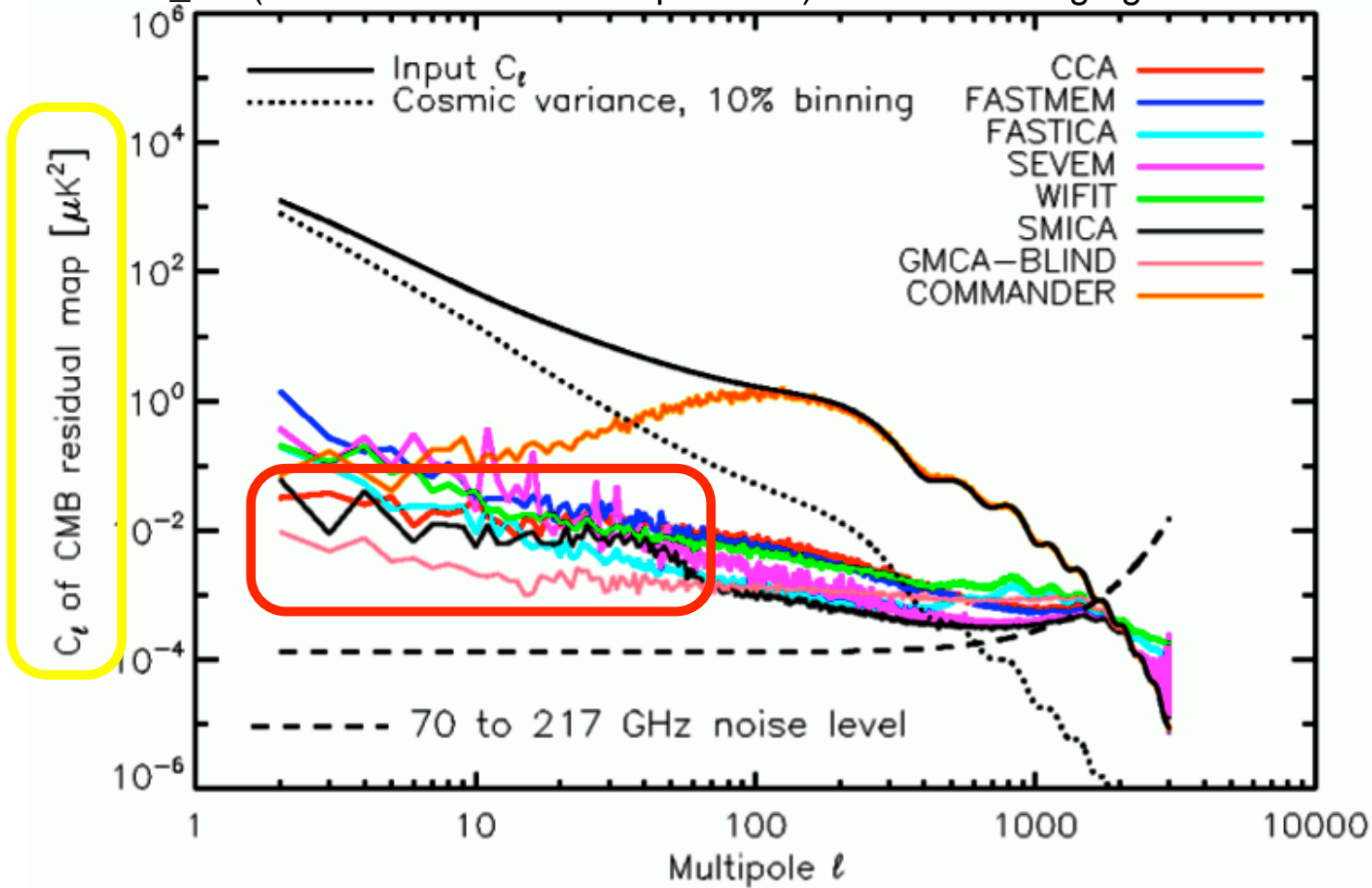
Estimated map with GMCA

Planck - WG2 - Challenger 2

comparisons - power spectrum

GMCA has the lowest spectral residuals at low l .

Plot shows C_l of (reconstructed CMB – input CMB) evaluated at high galactic latitudes.



■ Sam Leach (SISSA), June 19, 2008, WG2 meeting, Munich

Limitations

$$\text{GMCA Model: } Y = A X + N$$

But three main problems:

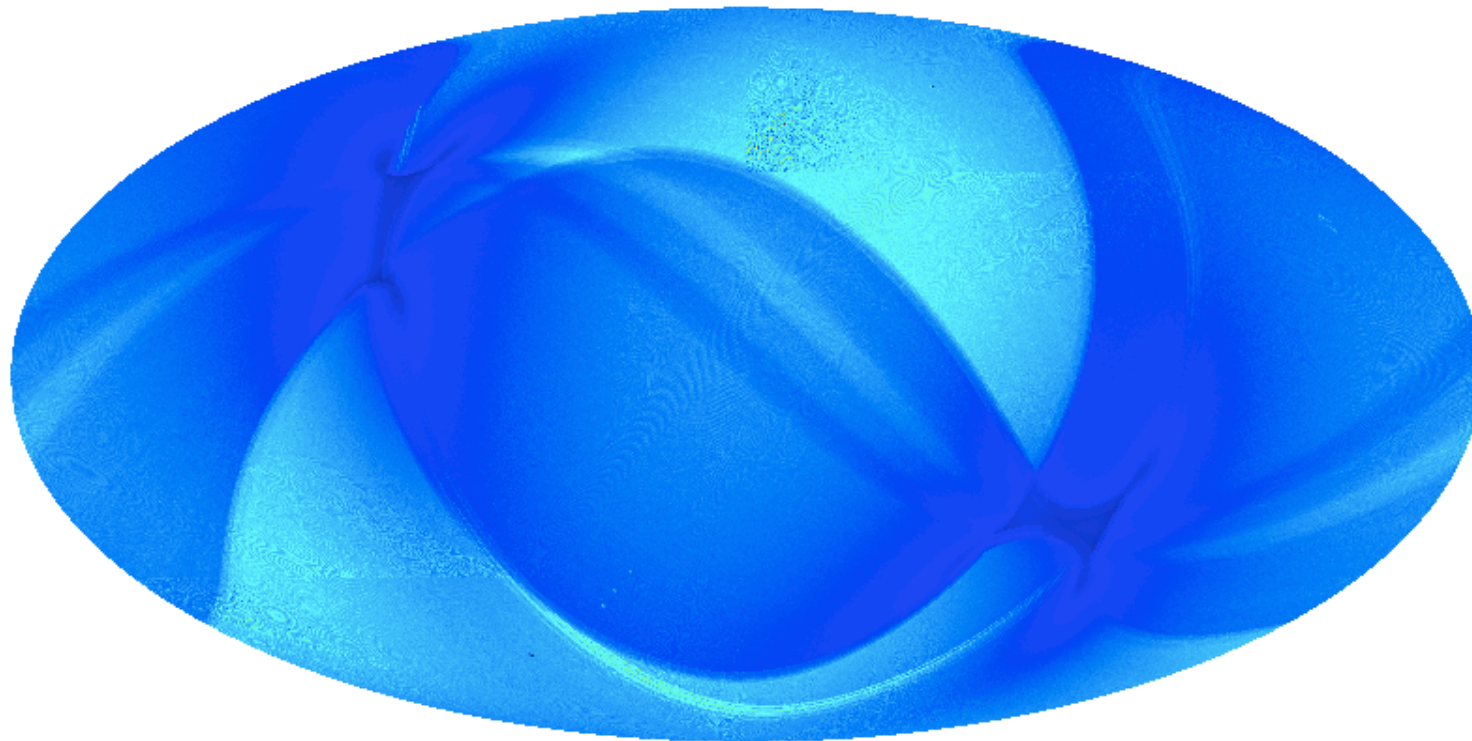
- i) A is spatially variant.
- ii) This model does not take into account the beam.
- iii) Noise is not homogeneous.

- Limitation of GMCA:

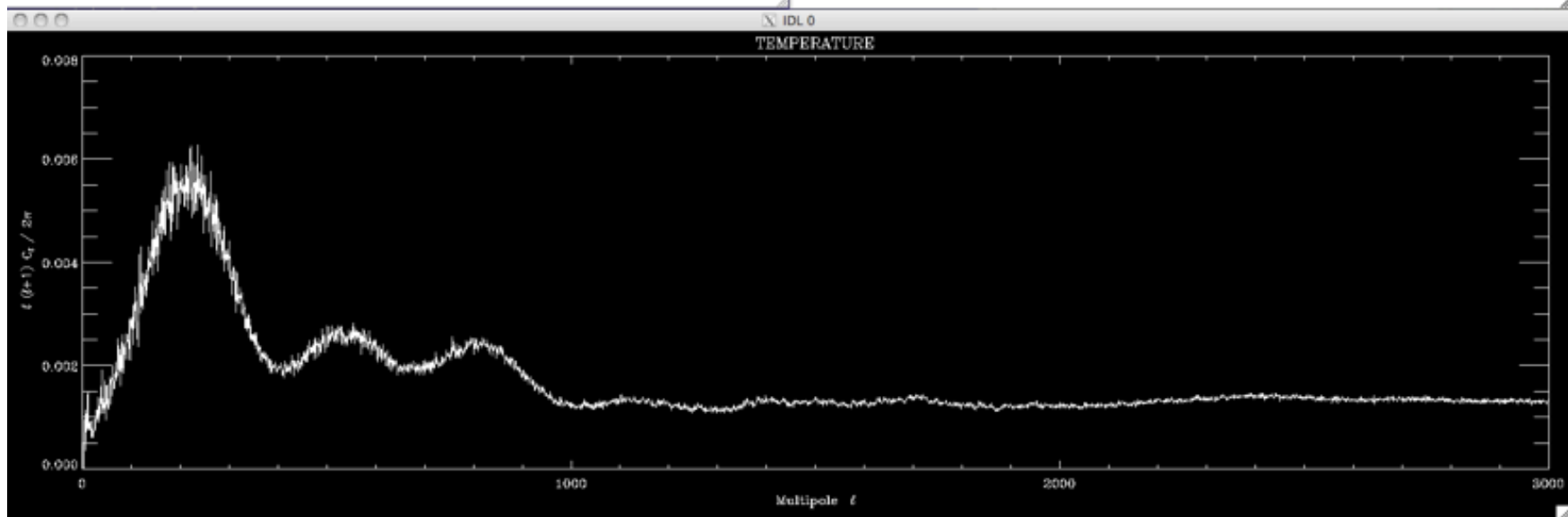
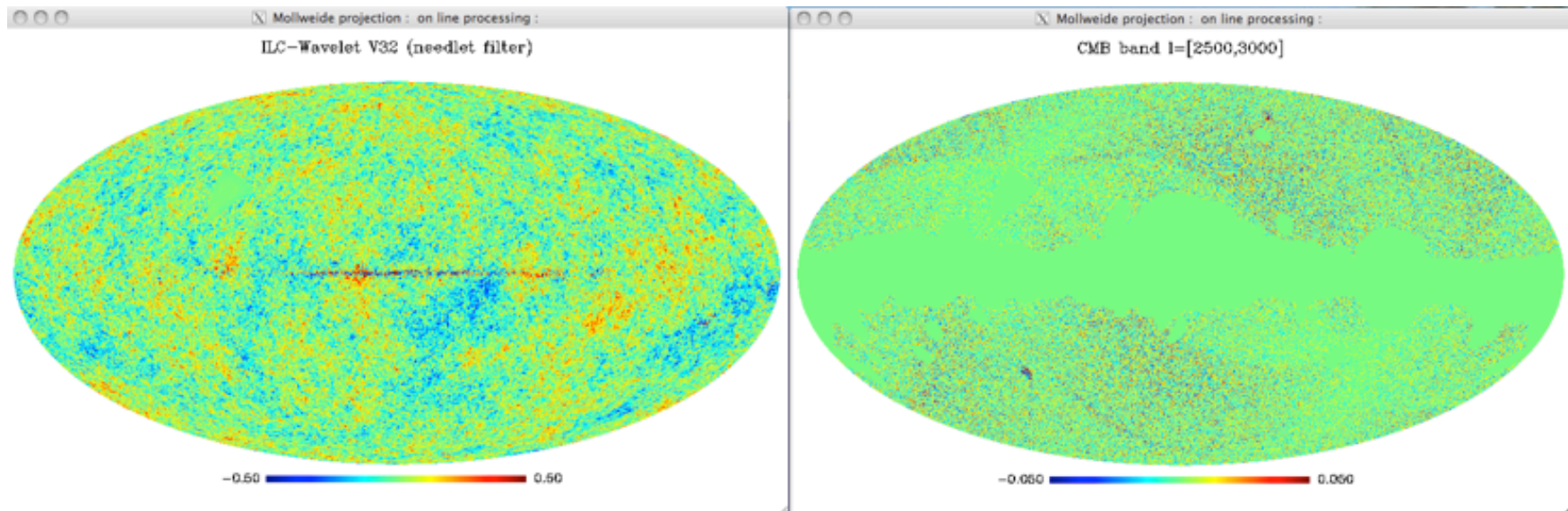
- * One matrix to describe the whole sky (i.e. the simplest model !)
- * PSF were not taken into account properly
- * Non stationary noise.

Non stationary noise problem

HFI GMCA RMS Map



0.0  0.27



Non stationary noise problem

The sparse inpainted solution was obtained by minimizing:

$$\min_{\alpha} \frac{1}{2\sigma^2} \|Y - A\Phi\alpha\|^2 \quad \text{s.t.} \quad \alpha \text{ is sparse}$$

A sparse inpainted and denoised solution can be obtained by minimizing:

$$\min_{\alpha} \frac{1}{2} \|Y - A\Phi\alpha\|_{\Sigma}^2 + \lambda \|\alpha\|^2 \quad \text{s.t.} \quad \alpha \text{ is sparse}$$

The notation $\|\cdot\|_{\Sigma}^2$ stands for the Frobenius norm of \mathbf{Y} in the noise covariance metric : $\|Y\|_{\Sigma}^2 = \text{Trace}(\mathbf{Y}^T \Sigma^{-1} \mathbf{Y})$.

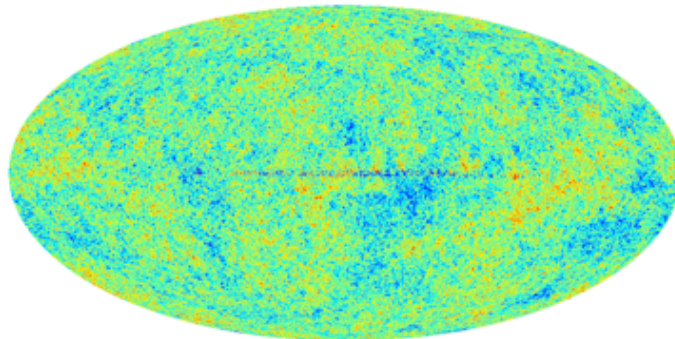
Forward-Backward Splitting Algorithm $\min_{\alpha} F_1(\alpha) + F_2(\alpha)$

Forward-backward splitting is a generalization of the classical gradient projection method for constrained convex optimization:

$$\alpha^{(n+1)} = \text{prox}_{\mu_n F_1} (\alpha^{(n)} - \mu_n \nabla F_2(\alpha^{(n)}))$$

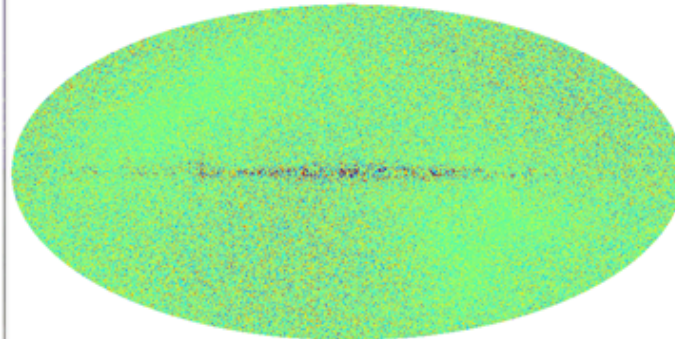
WG2 - Challenge 2

WG2-Challenge 2 GMCA-CMB Map



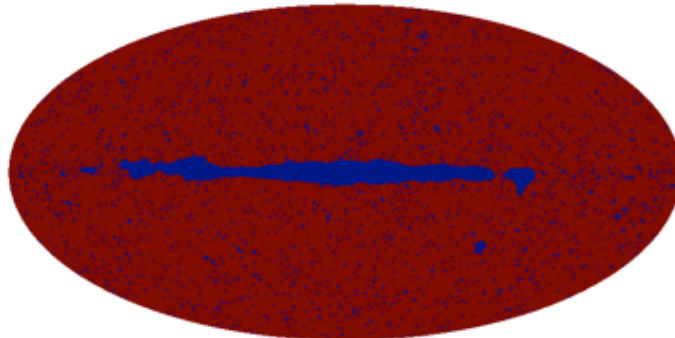
-0.50 0.50

Challenge 2 GMCA-MAP High Freq (l>2500)



-0.050 0.050

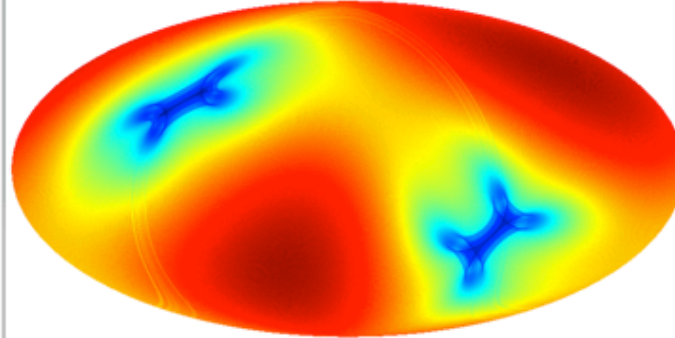
WG2 Mask: point sources + galactic plane



0.0 1.0

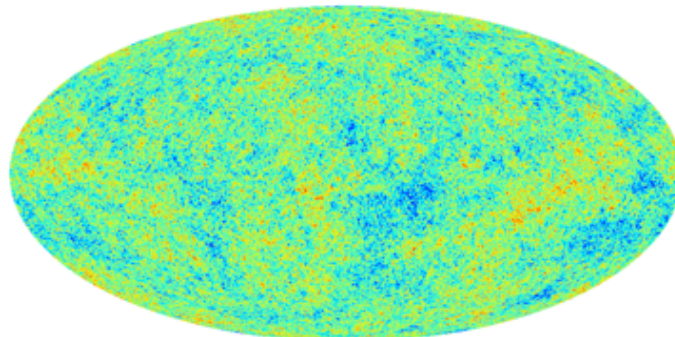
Mollweide projection : on line processing :

on line processing :



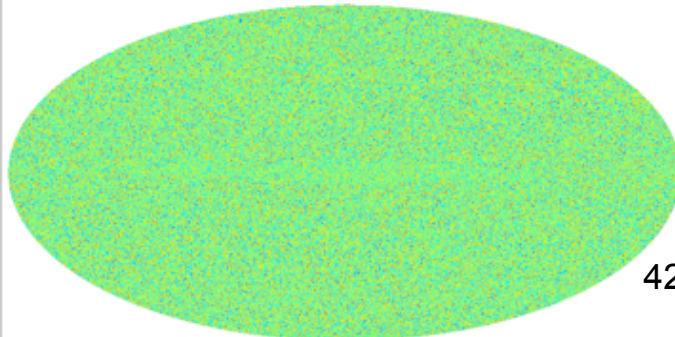
0.020 0.062

GMCA-CMB inpainted-Denoised Map



-0.50 0.50

Challenge 2 GMCA-Inpainted-Denoised MAP: High Freq (l>2500)



-0.0065 0.0065

The BEAM problem

- 1- Work in the spherical harmonic domain (SMICA)
- 2- Perform the component separation several times:
 - . one with all channels up to $l=300$,
 - . Repeat with less channels up to 500, 800, 1200, 3000.
 - . Merge all results

The second approach could be done in much more elegant way using the Wavelet-Vaguelette Decomposition (Donoho, 1995, Abramovich, 1998).

Wavelet-Vaguelette GMCA Decomposition

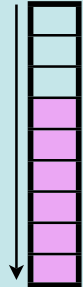
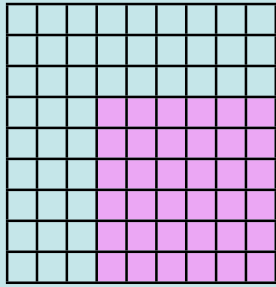
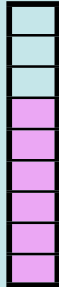
Inverse problem

$$y = Kf + n \xrightarrow{\text{WVD}} f = \sum_j \sum_k \langle Kf, \Psi_{j,k} \rangle \psi_{j,k} \quad \text{with } K^* \Psi_{j,k} = \psi_{j,k}$$

$$\tilde{f} = \sum_j \sum_k \Delta(\langle y, \Psi_{j,k} \rangle) \psi_{j,k}$$

Multi-channel WVD

$$Y_i = \sum_j K_i(A_j X)_i + N_i \longrightarrow \tilde{X}_s = \left[\sum_j \sum_k \tilde{A}_j^+ \langle Y_i, \Psi_{j,k}^{(i)} \rangle \psi_{j,k} \right]_s$$

$\beta_{j,k} = \langle Y_i, \Psi_{j,k}^{(i)} \rangle =$

 A_j

 $\alpha_{j,k} = \langle X_s, \psi_{j,k} \rangle$


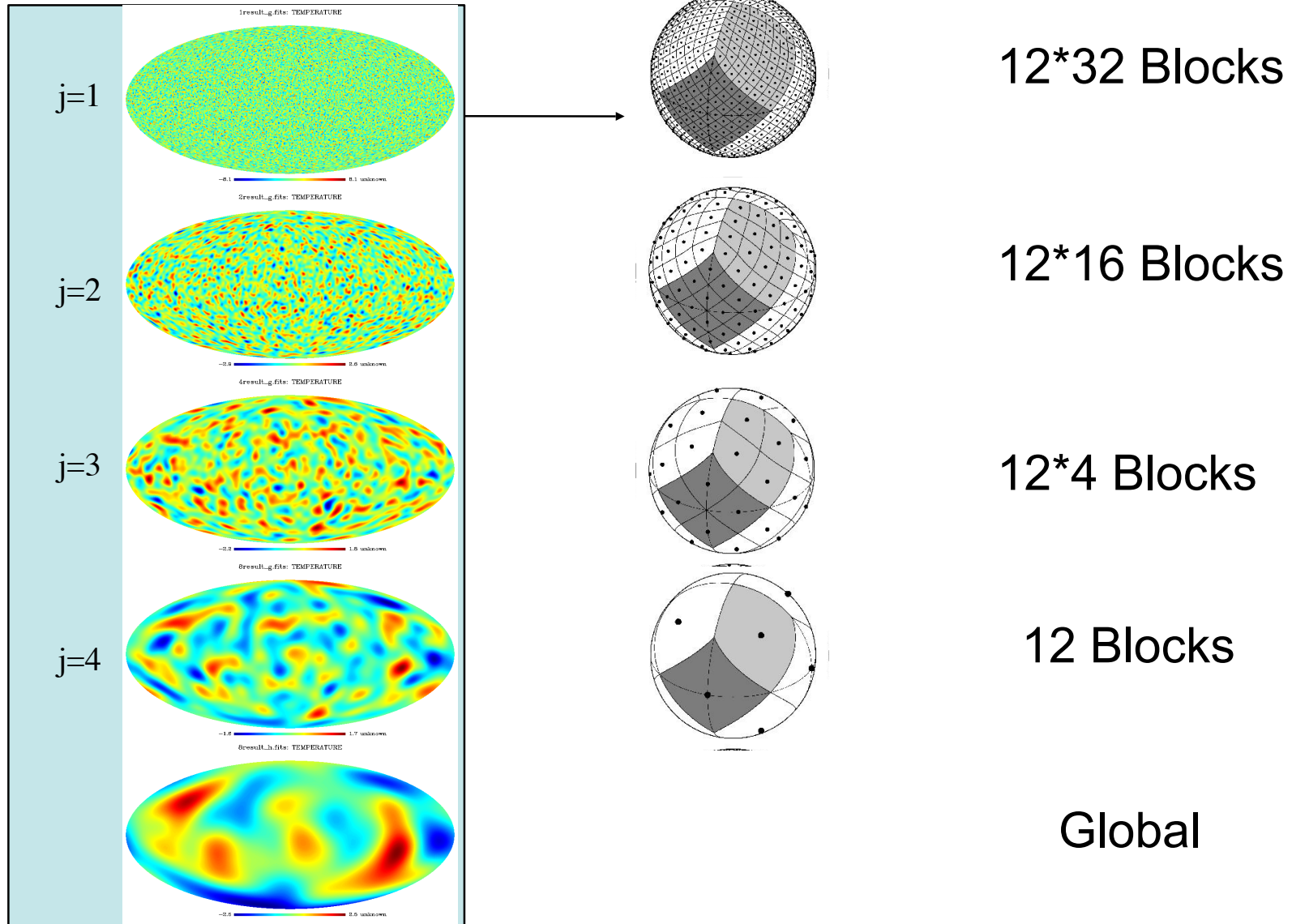
with $K_i^* \Psi_{j,k}^{(i)} = \psi_{j,k}$

The sparse GMCA solution is obtained by minimizing:

$$\min_{\alpha_j, A_j} \sum_j \frac{1}{2\sigma^2} \|\beta_j - A_j \alpha_j\|^2 \quad \text{s.t. } \alpha \text{ is sparse}$$

LOCAL GMCA

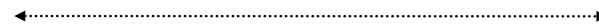
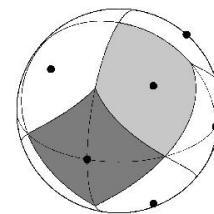
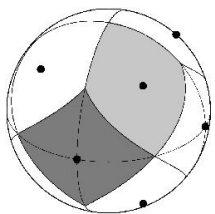
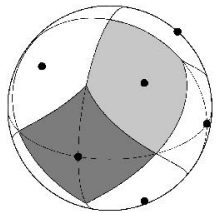
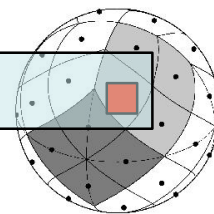
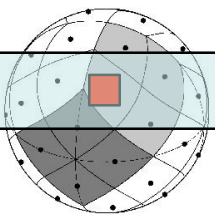
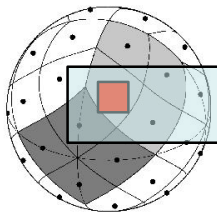
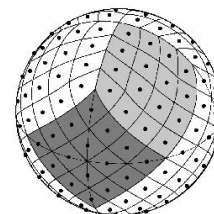
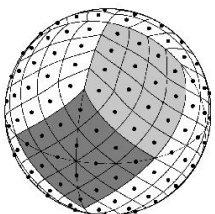
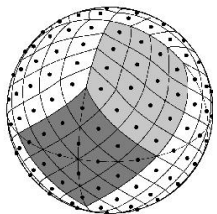
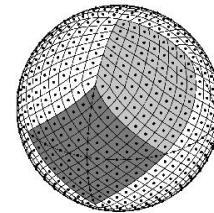
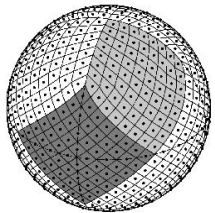
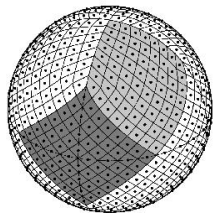
Undecimated Isotropic Wavelet Transform + Block Partitioning



Channel 1

Channel 2

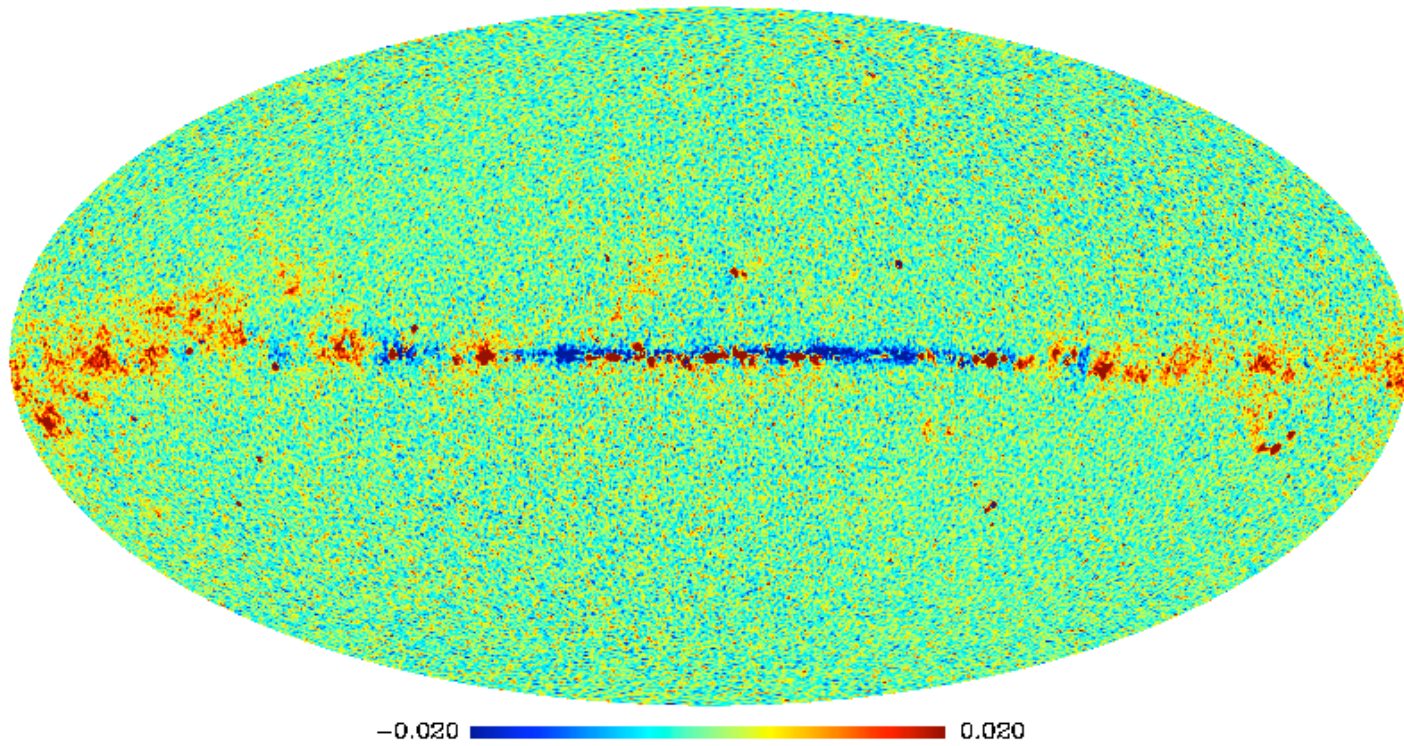
Channel 9



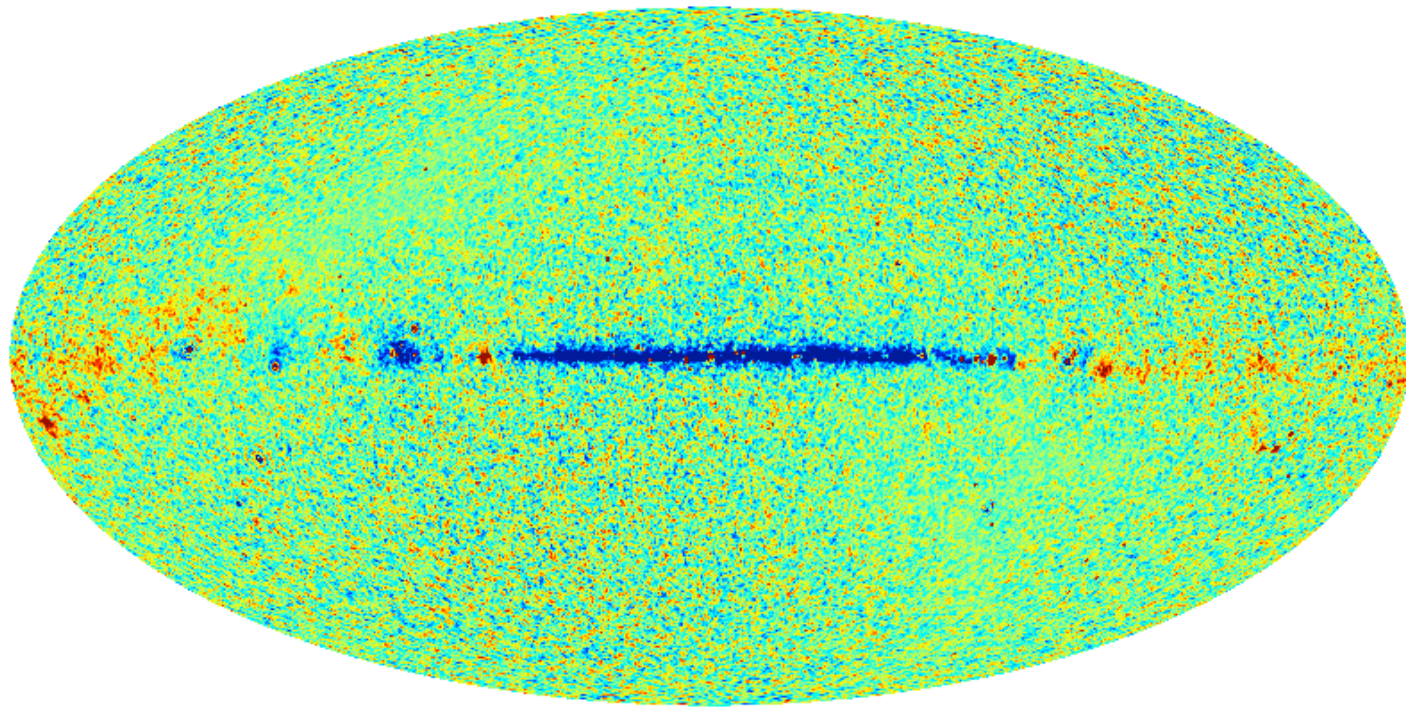
GMCA

GMCA - Global vs Patch v I

Global GMCA - 30 arcmin residual (en mK)

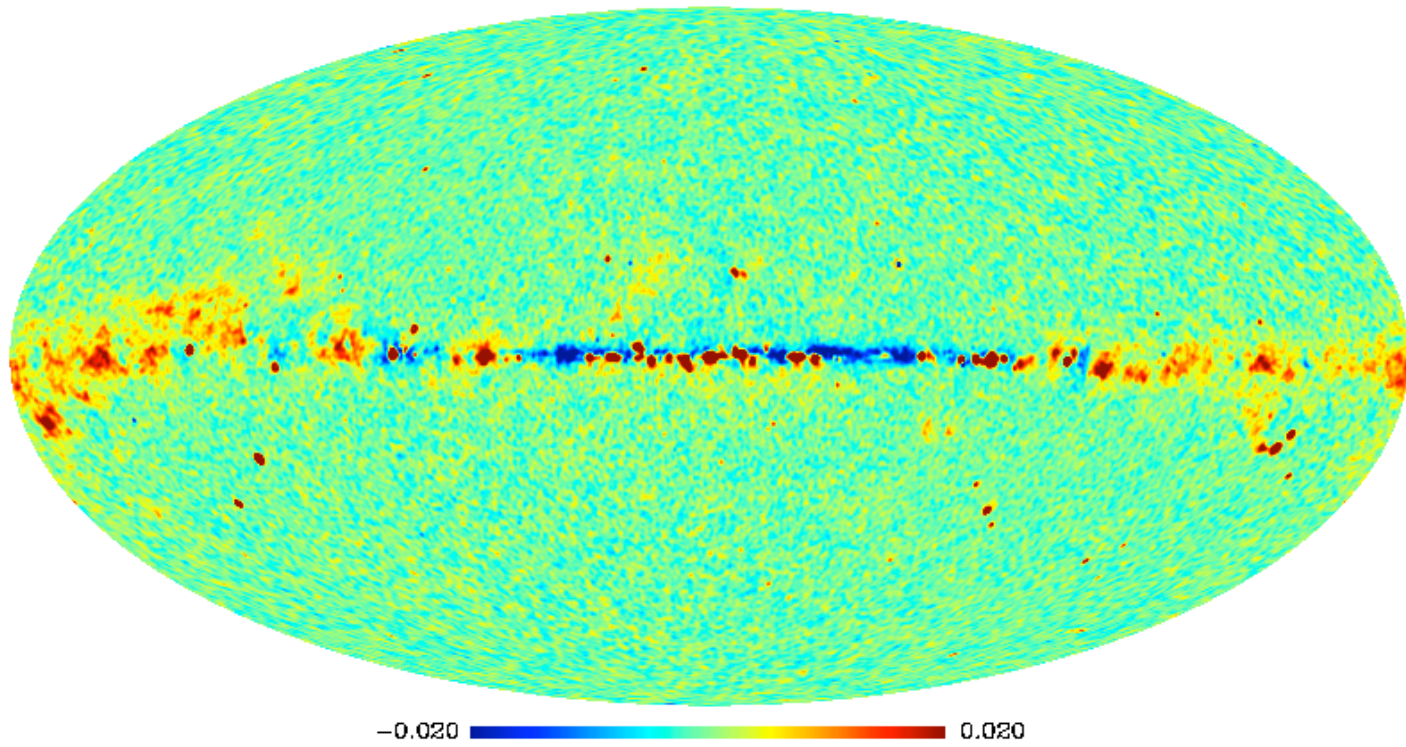


Patch-GMCA v1 - 30 arcmin residual (en mK)

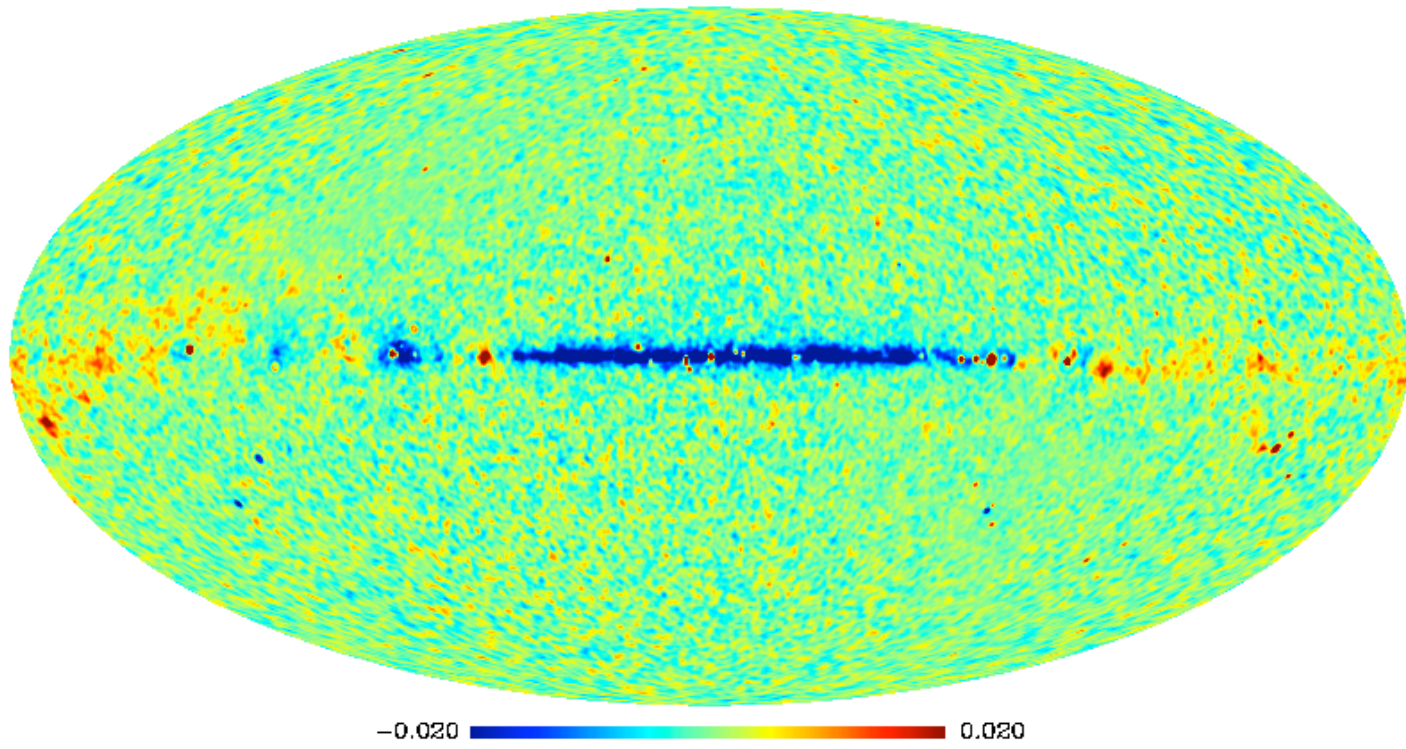


-0.020 0.020

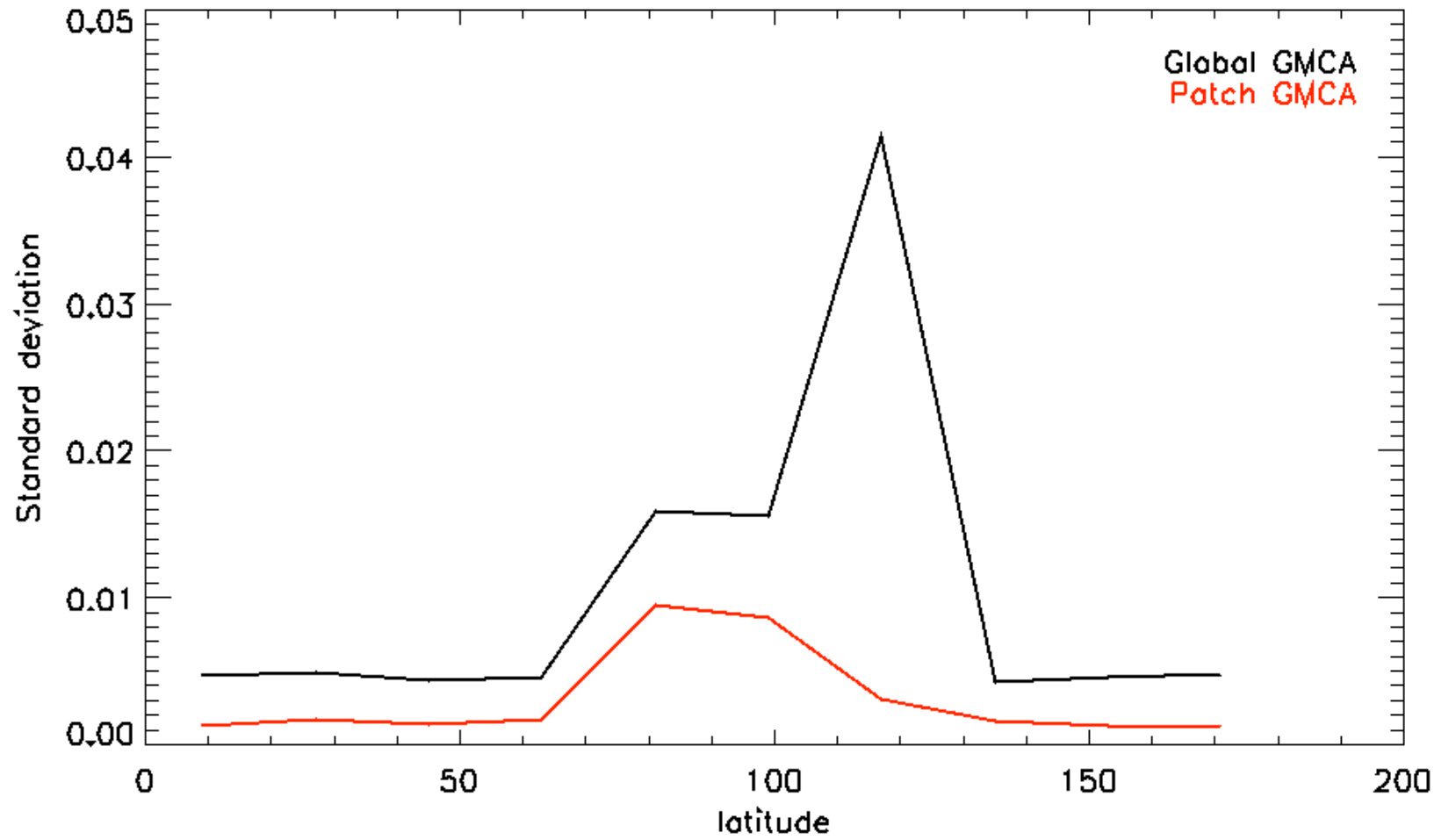
Global GMCA - 60 arcmin residual (en mK)

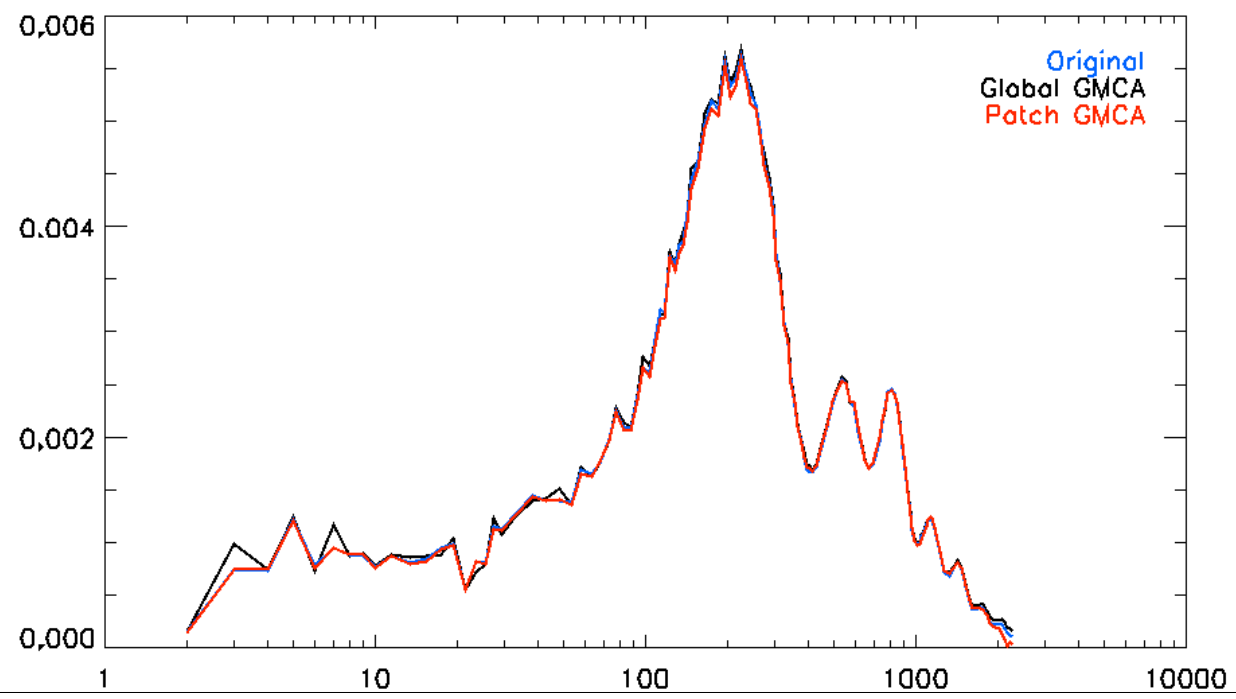
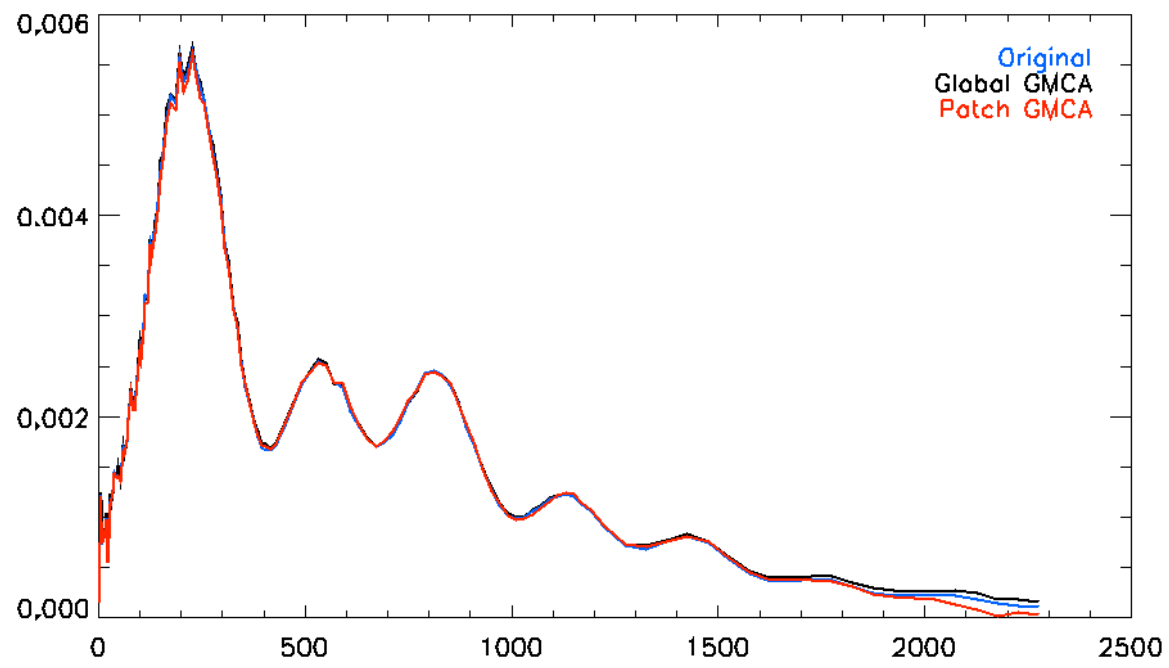


Patch-GMCA v1 - 60 arcmin residual (en mK)

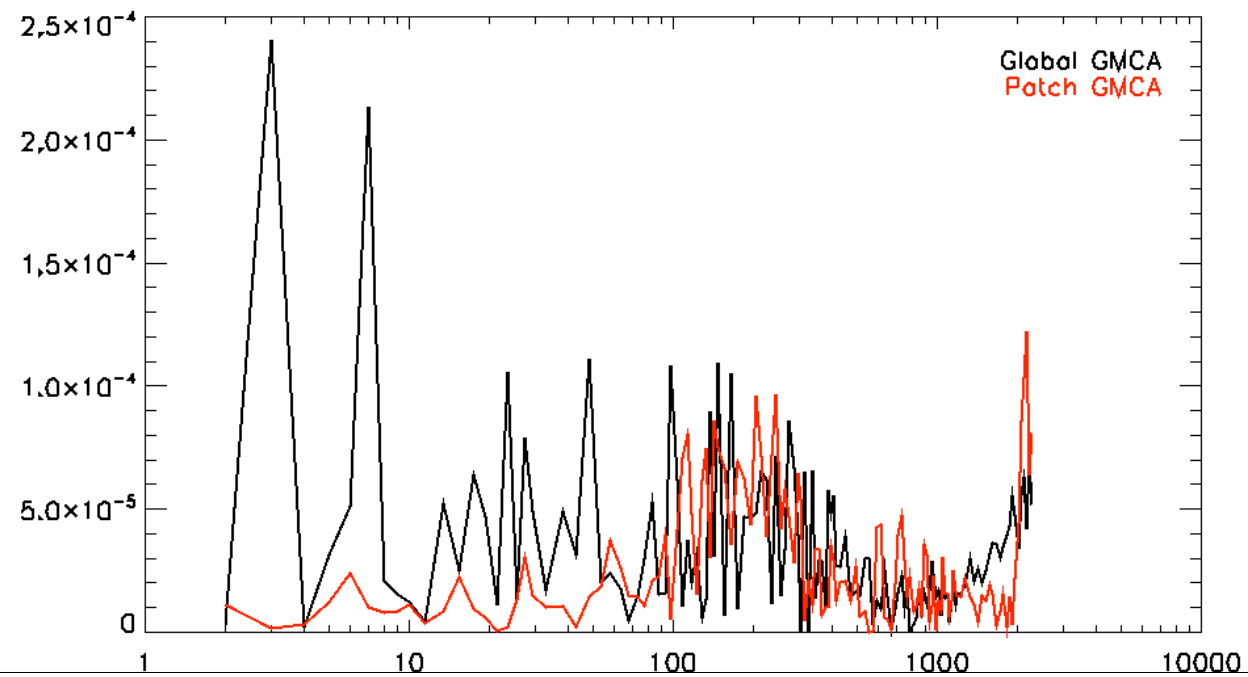
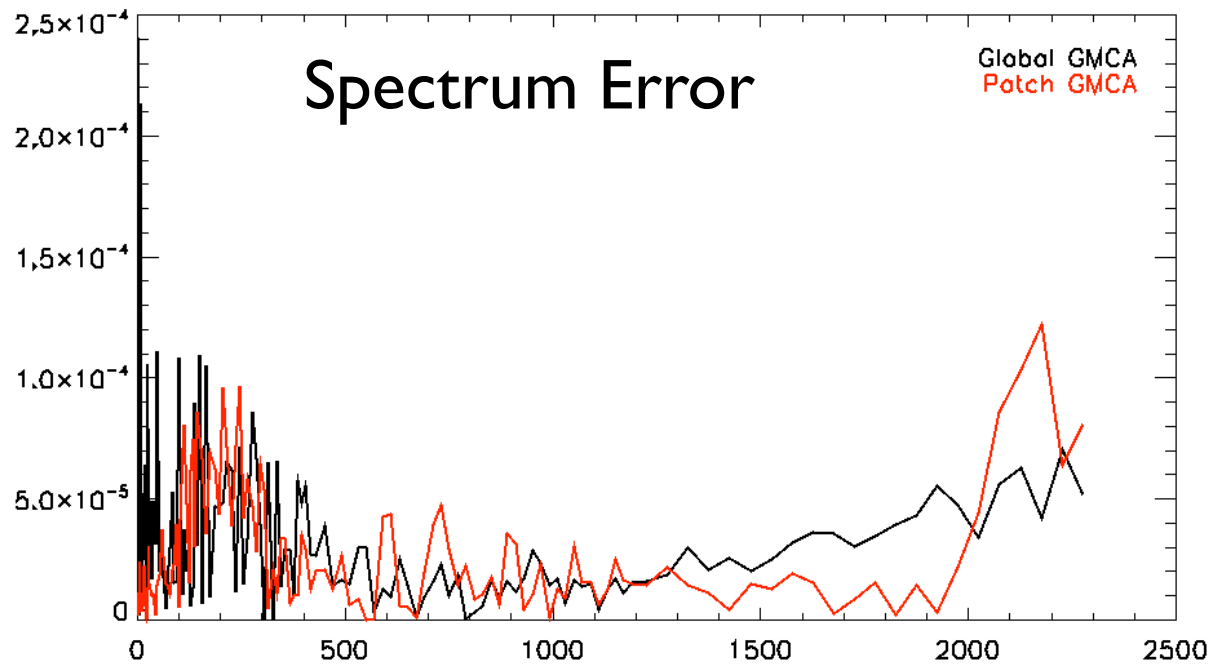


Quadratic Error per Latitude Band





Spectrum Error



PSM Sparse Reconstruction

Flexible Framework in Convex Optimization

- **Flexible Framework** developed in Convex Optimization

$$\underset{x \in \mathbb{R}^n}{\text{minimize}} \quad f_1(x) + \dots + f_m(x)$$

P. L. Combettes and V. R. Wajs, "Signal recovery by proximal forward-backward splitting", Multiscale Modeling and Simulation, vol. 4, no. 4, pp. 1168-1200, November 2005

F.X. Dupe, M.J. Fadili, J.-L. Starck, "A proximal iteration for deconvolving Poisson noisy images using sparse representations", IEEE Transactions on Image Processing, Vol. 18, No. 2

C. Chau, J.-C. Pesquet, N. Pustelnik, "Nested iterative algorithms for convex constrained image recovery problems", SIAM Journal on Imaging Sciences, Vol. 2, No. 2, Jun. 2009, pp. 730-762

- **Convex function to minimize:** F. Sureau, O. Fourt, and J.L Starck, ADA 6, may 2010.

$$\hat{\alpha}_c^{(n)} = \arg \min_{\alpha_c} \underbrace{\|Y - A\Phi\alpha_c\|_{\Sigma}^2}_{f_1} + \underbrace{\lambda\|\alpha_c\|_1 + i_C(\Phi\alpha_c)}_{f_2}$$

$$i_C(s) = \begin{cases} 0 & \text{if } s \in C \\ +\infty & \text{if } s \notin C \end{cases} \quad \text{to enforce constraints (positivity, bounds, support...)}$$

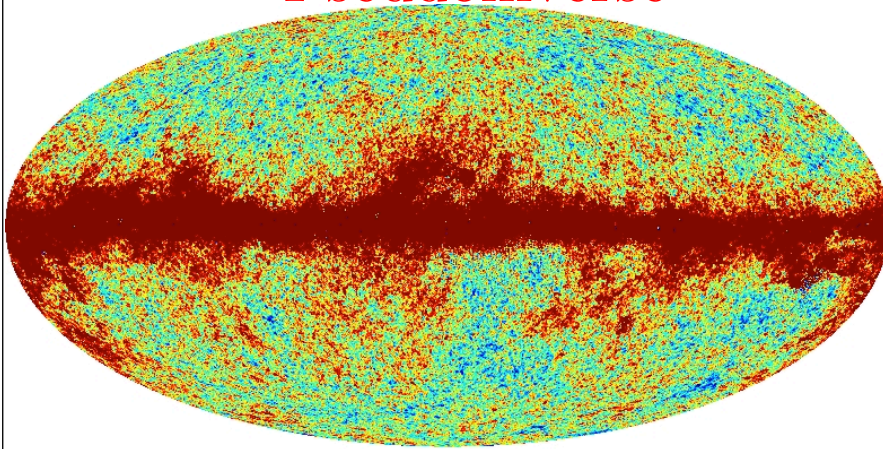
Toy Model Experiment

- **Toy model to evaluate if this approach is robust to error in A**
- Linear Model based on maps from the Planck Sky Model (CMB, Free/Free, Synchrotron, Spinning and Thermal Dust)
- No spatial variance of spectral indices
- Gaussian Beam and i.i.d noise according to Planck specifications
- Approximate mixing matrix by uniform error of 5% on A except for CMB (known)
- Sparsity constraint (Wavelets)
- Bounds on min/max values for each component, **map Nside=512**
- **Constraints in image space and wavelet space.**

Model: $Y = L X + N$, and we have an approximation of L

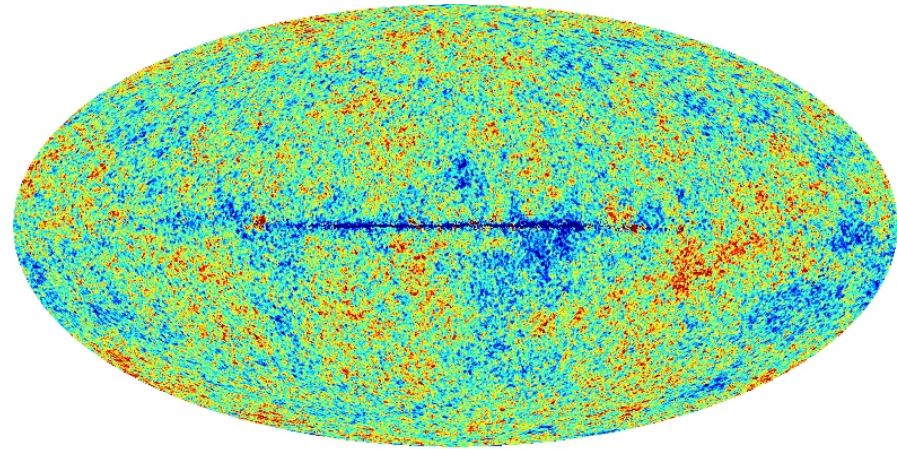
Results

Pseudoinverse



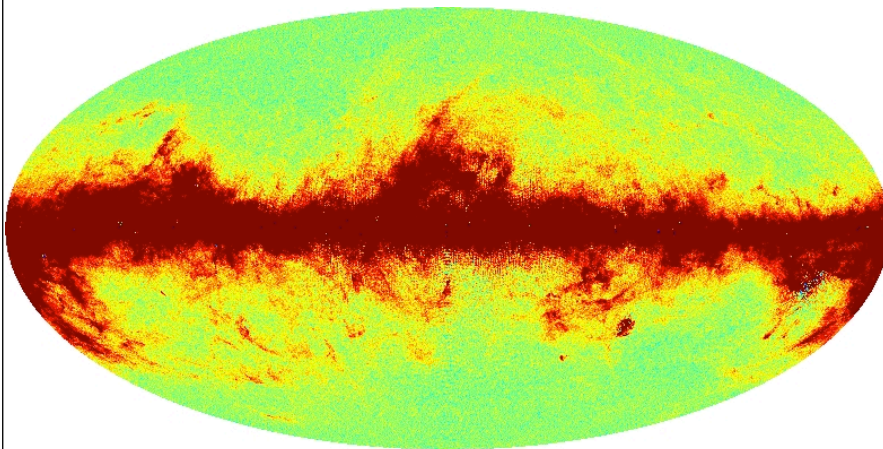
-0.30 0.30

Constrained restoration



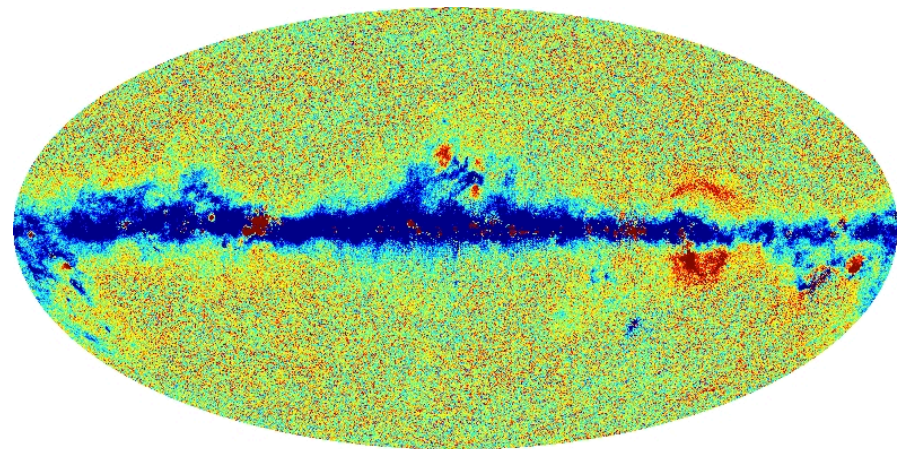
-0.30 0.30

Residual Pseudoinverse



-0.30 0.30

Residual Constrained Rest.



-0.030 0.030

Conclusions

- We have investigated another approach (i.e. sparsity) for PLANCK data analysis.
- Software available for sparse representation for both temperature and polarized maps.
- GMCA, the sparse component separation method, gives very interesting results a low l , with a simple model (a single matrix).

Perspectives

- We expect a strong improvement by using a more complex model (i.e. local GMCA, wavelet-GMCA decomposition).
- We need to extend it to take into account the polarization.
- We need to exploit better our knowledge of the galactic emission ==> MISTIC project.